Accepted Manuscript

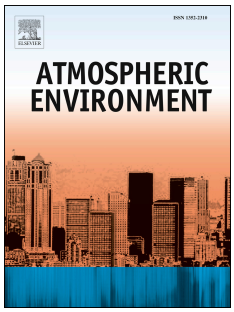

Global assessment of the effect of climate change on ammonia emissions from seabirds

S.N. Riddick, U. Dragosits, T.D. Blackall, S.J. Tomlinson, F. Daunt, S. Wanless, S. Hallsworth, C.F. Braban, Y.S. Tang, M.A. Sutton

PII: S1352-2310(18)30269-3

DOI: 10.1016/j.atmosenv.2018.04.038

Reference: AEA 15971

To appear in: *Atmospheric Environment*

Received Date: 31 August 2017

Revised Date: 20 April 2018

Accepted Date: 22 April 2018

Please cite this article as: Riddick, S.N., Dragosits, U., Blackall, T.D., Tomlinson, S.J., Daunt, F., Wanless, S., Hallsworth, S., Braban, C.F., Tang, Y.S., Sutton, M.A., Global assessment of the effect of climate change on ammonia emissions from seabirds, *Atmospheric Environment* (2018), doi: 10.1016/j.atmosenv.2018.04.038.

Global assessment of the effect of climate change on ammonia emissions from seabirds.

S. N. Riddick[1, 2, *] U. Dragosits[1], T. D. Blackall[2], S. J. Tomlinson[1], F. Daunt[1], S. Wanless[1], S. Hallsworth[1], C. F. Braban[1], Y. S. Tang[1] and M. A. Sutton[1]

[1] Centre for Ecology & Hydrology Edinburgh, Bush Estate, Midlothian, UK

[2] King's College London, Strand, London, UK

[*] now at Princeton University, Princeton, NJ, USA

Key Words: Seabirds; Global NH_3 emission; Process-based modelling, Climate change

Abstract

Seabird colonies alter the biogeochemistry of nearby ecosystems, while the associated emissions of ammonia (NH_3) may cause acidification and eutrophication of finely balanced biomes. To examine the possible effects of future climate change on the magnitude and distribution of seabird NH_3 emissions globally, a global seabird database was used as input to the GUANO model, a dynamic mass-flow process-based model that simulates NH_3 losses from seabird colonies at an hourly resolution in relation to environmental conditions. Ammonia emissions calculated by the GUANO model were in close agreement with measured NH_3 emissions across a wide range of climates. For the year 2010, the total global seabird NH_3 emission is estimated at 82 [37 - 127] Gg $year^{-1}$. This is less than previously estimated using a simple temperature-dependent empirical model, mainly due to inclusion of nitrogen wash-off from colonies during precipitation events in the GUANO model. High precipitation, especially between 40° and 60° S, results in total emissions for the penguin species that are 82% smaller than previously estimated, while for species found in dry tropical areas, emissions are 83 - 133% larger. Application of temperature anomalies for several IPCC scenarios for 2099 in the GUANO model indicated a predicted net increase in global seabird NH_3 emissions of 27% (B1 scenario) and 39% (A2 scenario), compared with the 2010 estimates. At individual colonies, the net change was the result of influences of temperature, precipitation and relative humidity change, with smaller effects of wind-speed changes. The largest increases in NH_3 emissions (mean: 60% [486 to -50] increase; A2 scenario for 2099 compared with 2010) were found for colonies 40°S to 65°N, and may lead to increased plant growth and decreased biodiversity by eliminating nitrogen sensitive plant species. Only 7% of the seabird colonies assessed globally (mainly limited to the sub-polar Southern Ocean) were estimated to experience a reduction in NH_3 emission (average: -18% [-50 to 0] reduction between 2010 and 2099, A2 scenario), where an increase in precipitation was found to more than offset the effect of rising temperatures.

1 Introduction

Several recent studies have reported that seabirds import significant amount of reactive nitrogen (N_r) from the ocean to the land and play an important role in local ecosystem nutrient cycling (Lindeboom, 1984; Blackall et al., 2008; Riddick et al., 2012). Nitrogen in guano excreted by birds changes chemically as it is

either incorporated into the soil organic matter, washed from the land surface or is emitted to the atmosphere as either ammonia (NH_3), nitric oxide (NO), nitrous oxide (N_2O) or diatomic nitrogen (N_2).

The formation of NH_3 from seabird guano is of particular interest, as NH_3 is a reactive gas that is readily incorporated into local ecosystems (Blackall et al., 2008), causing significant plant growth near to seabird colonies in otherwise nutrient poor regions (Lindeboom, 1984; Anderson and Polis, 1999). However, excess NH_3 can adversely affect the growth and also reduce plants' tolerance to pests, diseases and other environmental stressors (Stulen et al., 1998; Sutton et al., 2008; Sutton et al., 2011). It is well recognized that NH_3 can cause eutrophication and acidification of ecosystems resulting in a reduction of biodiversity (e.g. Sutton et al., 2011). In addition to near-source ecosystems, NH_3 emissions can adversely affect air quality through aerosol formation (Gu et al., 2014) and alter global climate as the aerosols affect the radiative forcing properties of clouds (Croft et al., 2016; Weber et al., 1998).

Previous studies have attempted to estimate the NH_3 emissions from seabird colonies globally. Blackall et al. (2007) applied a bioenergetics model, first developed by Wilson et al. (2004), to estimate a global NH_3 emission of 242 Gg NH_3 yr^{-1} from seabirds. One major shortcoming of this study was that it did not consider the effects of temperature. Ammonia release from a N_r source is highly dependent on temperature though according to Henry's Law and aqueous NH_3-NH_4^+ equilibria (Nemitz et al., 2001, Zhu et al., 2011, Riddick et al., 2016b). In the case of avian N_r excretion, which is mainly as uric acid, its hydrolysis to produce NH_3 is also both moisture and temperature dependent (Elliott and Collins, 1982). By not taking these interactions into account, the global emissions estimates of Blackall et al. (2007) must be considered as highly uncertain.

The effects of temperature on global NH_3 emissions from seabird guano were subsequently explored by Riddick et al. (2012), where the bioenergetics model of Blackall et al. (2007) was adapted using an empirical temperature correction. Riddick et al. (2012) estimated global emissions using a contemporary seabird population database for three scenarios: no temperature dependence (Scenario 1), full solubility dependence according to the thermodynamics of Henry's Law and aqueous ammonium dissociation (Scenario 2) and) a mid-range estimate between Scenarios 1 and 2 (Scenario 3). The total NH_3 emission for Scenario 1 was estimated at 442 Gg NH_3 $year^{-1}$, with penguins contributing 83% of the overall emissions. When full thermodynamic temperature dependence was assumed (Scenario 2), the total global NH_3 emission from seabirds was much lower at 97 Gg NH_3 $year^{-1}$, with penguins contributing 63% of the total emissions. Scenario 3 gave an intermediate estimate of 270 Gg NH_3 yr^{-1}. Riddick et al. (2012) considered that Scenario 3 represented the best-guess, as they anticipated that temperature was not the only limiting factor, with other environmental variables, such as precipitation and wind speed, also likely to affect NH_3 emission.

Even though Riddick et al. (2012) did not account for all environmental factors, they presented the first global map of NH_3 emissions from seabirds, demonstrating the extent to which seabird emission are remote from anthropogenic sources of N_r. Building on the earlier database of Blackall et al. (2007), the revised database by Riddick et al. (2012) spatially resolved 33,255 seabird colonies of 323 species in

180 countries. To address the shortcomings of the Riddick et al. (2012) emission estimate, a process-based approach was developed. First proposed by Blackall (2004) and later refined and tested by Riddick et al. (2017), the GUANO model (Generation of emissions from Uric Acid Nitrogen Outputs) is a dynamic mass-flow process-based model that simulates NH_3 losses from seabird colonies at an hourly resolution. The GUANO model was first applied for comparison with high- and low-temporal resolution measurements datasets (e.g. Blackall et al., 2007; Riddick et al., 2014, 2016a) of seabird NH_3 emissions in different parts of the world. The model application showed that the measured percentage of excreted N_r in guano that volatilizes as NH_3 (P_v) could be well reproduced at sub-polar, temperate and tropical seabird colonies by the GUANO model (Sutton et al., 2013; Riddick et al., 2017). The key climatic driver was found to be temperature, with precipitation, relative humidity and wind speed also influencing P_v.

The sensitivity of NH_3 emissions to environmental factors, as clearly demonstrated in measurements (Sutton et al., 2013, Riddick et al., 2014, 2016b), suggests that global climate change over time will affect NH_3 emissions from seabird colonies throughout the world. According to the Intergovernmental Panel on Climate Change (IPCC, 2007), average global surface temperature has been estimated increase by between 1.1 and 6.4 °C by 2100, with global average precipitation changing by up to ± 20 %, a broad scale of change that has since been supported by the IPCC 5th Assessment Report (IPCC, 2013). As many colonies of penguins and other seabird species exist in delicately balanced, pristine environments with low anthropogenic emissions, potentially large changes in NH_3 emissions over the next 90 years could have a pronounced environmental impact in these remote regions.

The present paper describes an adaptation and application of the colony based GUANO model (Riddick et al., 2017) to calculate NH_3 emission estimates from all seabird colonies detailed in the global seabird database collated by Riddick et al. (2012). The model output provides a new best estimate of current global NH_3 emissions from seabirds and a new spatial distribution of emissions which we compare with our previous estimates. We then apply the model using temperature, precipitation, relative humidity and wind speed anomalies for a selection of 2099 climate scenarios from IPCC (2007) as a basis to assess how future climate change may affect the distribution and global magnitude of seabird NH_3 emissions.

2 Methods & Materials

2.1 GUANO Model

For each seabird colony in the global seabird population database (Riddick et al., 2012), we applied the GUANO model (Riddick et al., 2017), using data on meteorology and bird metabolism to calculate hourly NH_3 emissions (F_H, g NH_3 m^{-2} h^{-1}) for a period of two years. A two-year simulation was used to calculate the annual emission (F_T, g NH_3 m^{-2} $year^{-1}$) as the sum of hourly emissions for the second year. In this way, the model was able to take account of uric acid deposited in the previous year that has not volatilized or been washed off by precipitation during winter and wet seasons (Blackall et al., 2008). A one-year spin-up time was used because at the colonies where guano builds up, there is either insufficient water to convert uric acid to TAN or it is not warm enough for

the TAN to volatilize. In both cases NH_3 emission does not increase in the 3rd year as the meteorology is repeated, with dry climates remaining dry and cold climates staying cold.

The GUANO model, which is described in detail by Riddick et al. (2017), was converted from a single-site based application (originally implemented in Microsoft Excel) to a script in R to enable large numbers of colonies to be processed at an hourly time resolution. Each colony was simulated independently of the others, i.e. there was no influence in the model of one colony on another.

2.2 Model Input

2.2.1 Nitrogen excretion rates

The average nitrogen excretion rate (N_e, g m^{-2} $hour^{-1}$) for each seabird species used in the GUANO model is calculated from the period of attendance at the colony (T, days), the proportion of the time spent at the colony during the breeding season (f_{tc}), the number of breeding adults per square meter (D_A, birds m^{-2}), the amount of nitrogen excreted per breeding adult ($F_{e\text{-}br}$, g $bird^{-1}$ day^{-1}), the amount of nitrogen excreted per chick ($F_{e\text{-}ch}$, g $chick^{-1}$ $year^{-1}$) and the productivity of the species (P, fledged chicks per breeding pair).

$$N_e = \frac{(1.167 T f_{tc} F_{e-br} D_A) + \left(F_{e-ch}\left(\frac{P}{2}\right) D_A\right)}{24T} \quad (1)$$

The amount of nitrogen excreted per breeding adult ($F_{e\text{-}br}$, g $bird^{-1}$ day^{-1}) and the amount of nitrogen excreted per chick ($F_{e\text{-}ch}$, g $chick^{-1}$ $year^{-1}$), Equation 2 and Equation 3, are calculated using the method of Wilson et al. (2004) from the adult mass (M, g $bird^{-1}$), the mass of the chick at fledging ($M_{fledging}$, g), nitrogen content of the food (F_{Nc}, g N g^{-1} wet mass), energy content of the food (F_{Ec}, kJ g^{-1} wet mass), assimilation efficiency of ingested food (A_{eff} , kJ [energy obtained] kJ^{-1} [energy in food]).

$$F_{e-br} = \frac{9.2.\, M^{0.774}}{F_{Ec} A_{eff}} F_{Nc} \quad (2)$$

$$F_{e-ch} = \frac{28.43 M_{fledging}^{1.06}}{F_{Ec} A_{eff}} F_{Nc} \quad (3)$$

F_{Nc} and F_{Ec}, estimated at 0.036 g N g^{-1} and 6.5 kJ g^{-1} (both wet mass), (Energy: Nitrogen (E:N) ratio = 181 kJ g N^{-1}) respectively, have been calculated assuming a high protein, fish only diet (Furness, 1991). A_{eff} is estimated at 0.8 (Furness, 1991).

Species-specific values for input parameters (adult mass, number of days spent at the colony per year, proportion of time at the colony, breeding success, fledging mass of the chick and breeding substrate) were extracted from the literature and are summarised in Appendix 1 of Riddick et al. (2012). Of the 318 species of seabird considered, species specific parameter data were available for 311 species (Birdlife International, 2017). Data for the missing species were estimated from similar species identified using Birdlife International (2017).

In its present form, as used in this paper, the global seabird database of Riddick et al. (2012) includes an updated population estimate (261 million breeding pairs, including data from 1984 to 2010). The database details seabird colonies at 33,255 locations, with the resolution of colony counts and details varying greatly between countries, from 878 colonies described for the UK (Scotland, Wales, Northern Ireland and England) to a single summary country population values for each of Nigeria, Uruguay and Haiti. As these different levels of detail in the data cannot easily be shown graphically, the maps in the results section aggregate up to a five degree resolution.

2.2.2 Parameterization of hourly air temperature

To calculate NH_3 emission accurately, the GUANO model requires hourly values for air temperature. For the reasons described in Supplementary Material Section 1, this study used a model based on Parton and Logan (1981) to calculate diurnal changes in air temperature given a maximum and minimum value. This temperature model calculates the air temperature at 2 m above the surface for each hour day (H) from the day of year (D), latitude (L, °), maximum temperature (T_{max}, °C) and minimum temperature (T_{min}, °C), using a sinusoidal relationship (Parton and Logan, 1981). A comparison of the diurnal air temperatures derived from Parton and Logan (1981) with measured values is presented in Supplementary Material Section 1.

2.2.3 Meteorological data

The GUANO model requires hourly input data for ground temperature, relative humidity, wind speed and precipitation. Data from the National Climatic Data Center (NCDC) Global Surface Summary of the Day (GSOD) data (NCDC, 2011) was used as it matched most closely to the data observed during the measurement campaign of Riddick et al. (2014; 2016a) (Supplementary Material Section 2). The daily average values presented in the GSOD dataset were used for relative humidity and wind speed. Hourly values for precipitation were calculated from the daily total divided by 24. Hourly air temperature values were calculated from the daily maximum and minimum using the method described above in 2.2.2, ground temperature data are not readily available and, therefore, were derived from air temperature, as described in Section 2.2.4.

2.2.4 Ground Temperature Modelling

In the absence of suitable global data for ground surface temperature (Supplementary Material Sections 2 & 3), this was derived from air temperature data for each colony, using surface and air temperature data from the three field work sites measured during the campaigns of Riddick et al. (2014, 2016a) to parameterize a temperature offset (T_o) function (Supplementary Material Section 3). For each seabird colony, T_o was calculated from the difference between air and ground temperatures measured during field campaigns at: the equator = T_o (Ascension Island; Riddick et al., 2014), 55 °N = T_o (Isle of May; Riddick et al., 2016a) and 55 °S = T_o (Bird Island; Riddick et al., 2016a). Using these measurements, T_o was derived for each seabird colony at each hour at any given latitude based on linear interpolation between latitudes of these hourly values.

Due to the relatively simple derivation method and the limited number of measurement sites, there is substantial uncertainty associated with the estimated

surface temperature. Based on daily variations in ground temperature at the three measurement sites, a best estimate of uncertainty in derived ground temperature at these sites is ± 1 °C. However, the global interpolation of these values must be acknowledged to be more uncertain, and probably ± 2 °C as a best estimate.

2.2.5 Assigning meteorological stations to seabird colonies

The geographically closest meteorological data in the GSOD database to each seabird colony were identified and extracted using a GIS. These meteorological data were used in the GUANO model to calculate NH_3 emissions for a base year of 2010. For colonies farther than 1000 km from a measurement site, the meteorological data were calculated as the average of the nearest three sites. The cut off of 1000 km was used because it was assumed that, for our purposes, climate at sea level would be sufficiently similar to sites within this distance. This correction was only necessary for 50 colonies out of the total of 33,255 colonies (<0.2%), mostly in the South Pacific and around Antarctica.

2.3 Analysis of meteorological effects

In order to investigate the relative effects of meteorology on NH_3 emission, relationships were fitted using a multiple regression model. Correlations between NH_3 emissions and the hourly meteorological data for each variable (air temperature, relative humidity, wind speed and precipitation as presented in the GSOD dataset) were identified by calculating the product moment correlation coefficient (r).

2.4 Climate change scenarios

Data from the IPCC Special Report on Emissions Scenarios (IPCC, 2007) were used to simulate potential future changes in NH_3 emissions from seabirds for different climate change scenarios. The specific scenarios used were: the best-case scenario (B1), the middle scenario (A1B) and the worst-case scenario (A2) (Mann & Kump, 2008). Scenario-specific data are available from the IPCC data distribution centre (IPCC Data, 2017) and were chosen because it provided anomaly data on temperature, northward and eastward wind components, precipitation and humidity for 2099 on a 2.5° by 3.75° grid.

The geographically closest anomaly data for each seabird colony were extracted using a GIS and added to the meteorological data in the GUANO model for the year 2099. It should be noted that no account was taken of potential effects of climate change on seabird populations that might occur due to changes in food availability or physical changes to breeding sites, e.g. sea level rise or increased storm frequency.

3 Results and Discussion

3.1 Global distribution of seabird NH_3 emission

The GUANO model application based on 2010 estimated total NH_3 emission at 81.8 Gg NH_3 $year^{-1}$, with large emissions in hotspots throughout the world, especially on tropical and sub-polar islands (Figure 1). It may be noted from Figure 1 that seabird species sometimes occur inland, for example cormorant colonies in Central Asia. The resulting distribution may be compared with the three empirical scenarios of temperature dependence mapped by Riddick et al. (2012): emissions assumed to be independent of temperature (Scenario 1: 404 Gg

NH_3 $year^{-1}$), emissions assumed to follow thermodynamically adjusted bioenergetics (referred to subsequently as the TABE model) (Scenario 2: 83 Gg $year^{-1}$) and the mid-estimate between these two (Scenario 3: 244 Gg $year^{-1}$). Overall, the GUANO model is found to agree most closely with the TABE model estimate of Riddick et al. (2012) (Scenario 2), pointing to a lower estimate of global emissions than what their best guess (Scenario 3). This similarity to Scenario 2 should, however, be considered as partly fortuitous, since the GUANO model uses a process based approach, compared with the empirical fit to measurements of Riddick et al. (2012), which does not include the effects of precipitation, relative humidity and wind. The consequence is that the spatial patterns of NH_3 emission across the world are also very different between this new dataset and the TABE model results.

Geographically, the main differences between the GUANO model and the TABE model are for the sub-polar latitudes (40 °S - 60 °S), where the TABE model emissions are twice as large as the GUANO model emissions (Supplementary Material Section 5 Figure SM5.1). These emissions are generally from the penguin colonies in the Southern Ocean, where temperatures are relatively low and precipitation is high, and the difference may be caused by unvolatilized nitrogen remaining on the ground longer before it is washed away by precipitation.

Between 15 °N and 25 °S, NH_3 emissions calculated by the GUANO model are higher than those calculated by the TABE model (Supplementary Material Section 5 Figure SM5.1). Both models incorporate an exponential relationship between temperature and NH_3 emission. However, the larger emissions in the tropics may be caused by the use of hourly ground temperature values in the GUANO model instead of an average value for the breeding season in the TABE model. The peaks during the day result in a higher P_v and exponentially larger emissions which are reflected in the larger annual emissions and average P_v (average tropical P_v for the GUANO model is between 10 and 15% higher than the average tropical TABE model P_v) at seabird colonies in the tropics (Supplementary Material Section 5 Figure SM5.1).

<<Insert Figure 1>>

A detailed comparison of the estimates from the GUANO and TABE models for 13 regions of the world is given in Supplementary Material Section 4 (Table SM4.2). Generally, NH_3 emissions calculated by the GUANO model are larger than the TABE model from colonies in the tropics in areas such as Australasia (72% larger) and the Indian Ocean (117% larger). However, NH_3 emissions calculated by the GUANO model are smaller than the TABE model from colonies in colder, wetter areas, such as Antarctica (35% smaller). As noted above, this is caused by the GUANO model taking into account nitrogen wash-off from the colony as a consequence of precipitation. The largest regional difference between the TABE and GUANO modelled NH_3 emissions is in Asia where the GUANO model predicts emissions 4.8 times larger. The TABE and GUANO model emissions were calculated using the same input bird data and the most noticeable difference in emissions is in the colonies around the Sea of Okhotsk (Supplementary Material Section 5 Figure SM5.3). As explained above, the exponential relationship between temperature and NH_3 emission in the GUANO

model uses hourly values of ground temperature, resulting in exponentially larger emissions. As the TABE model uses average temperature during the breeding season rather than daily varying temperature, the exponential relationship would tend to give higher emissions in the GUANO model in the warmest areas.

3.2 Analysis of meteorological effects on NH_3 emissions

The relationships of temperature, relative humidity, wind speed and precipitation were compared to the P_v estimates derived from the GUANO model for the breeding season at all global colonies (Supplementary Material Section 5 Figure SM5.3). Given that there is no strong correlation between the different meteorological variables themselves (Supplementary Material Section 5 Table SM5.1), we applied a multiple regression model to establish their relative importance to P_v. The multiple regression model between meteorological parameters is based on averaged values, where daily averaged data was used as hourly data for relative humidity and wind speed. Hourly precipitation is the daily total precipitation divided into 24 equal hourly values and the hourly temperature is the hourly ground temperature as calculated by the method in Supplementary Material Section 3. The multiple regression model indicates that, modelled across the sites, P_v is most sensitive to temperature and precipitation (Supplementary Material Section 5 Table SM5.2). Warmer conditions favour an increase in P_v, while wetter conditions, which includes the effects of relative humidity, with more precipitation favour a smaller P_v. Wind speed has the least effect on P_v of the four variables included, however the relationship is positive and wind speed clearly affected measured emissions at some sites, especially Bird Island (Riddick et al., 2016a). In strong winds, both aerodynamic and boundary-layer resistances are reduced and the rate of emission increases. However, wind speed only limits the rate of transport of NH_3 from the ground and the magnitude of wind speed has no effect on the rate of NH_3 production.

The relationships between meteorological variables and P_v can be explained by considering how uric acid evolves to form NH_3. Ammonia emission increases with temperature because of decreased solubility of NH_3 on the surface described by Henry's Law. The TABE model does not take into account uric acid, TAN and non-volatilized NH_3 washed away during precipitation events. It is difficult to parameterize N run-off because of differences in speed and efficiency in wash-off of guano from different nesting habitats (such as rock, sand, burrows) and slopes. Like temperature, increases in relative humidity increase the amount of uric acid that converts to TAN because of increased hydrolysis, which would explain the significant relationship between relative humidity and NH_3 emission.

The effects of meteorology on P_v can explain why the global seabird NH_3 emission calculated using the GUANO model is lower than previous estimates. The TABE model (Riddick et al., 2012 - Scenario 2) estimates that 65 % of global NH_3 emissions are due to penguin species, compared with 42% according to estimates using the GUANO model. This smaller contribution by penguins can be explained by temperature reducing the amount of NH_3 evolved from uric acid at these sites. Due to the penguin colonies' location on cold and wet Sub-Antarctic islands, TAN is formed only slowly from uric acid, resulting in low NH_3 emission rates. Coupled with this, precipitation events reduce the presence of uric acid,

TAN and NH_3 at the surface due to run-off, thereby decreasing the overall percentage of excreted nitrogen that is available for volatilization.

The largest populations of seabirds are found in Antarctica and the Southern Ocean, and because of their relatively large mass, these are also the species excreting the most nitrogen (Riddick et al., 2012). On a global scale, seabird N excretion is dominated by Antarctica and the Southern Ocean, which account for 79 % of the total excreted. However, the meteorology (low temperatures and high precipitation) at these colonies reduces emissions to relatively small values, thus only 34.2 Gg NH_3 $year^{-1}$ are emitted from the 858.2 Gg N $year^{-1}$ excreted in Antarctica and the Southern Ocean (P_v = 4 %) (Figure 2). By contrast, NH_3 emissions from the tropics are relatively high compared with the total amount of N excreted, mainly due to hot temperatures. For example, seabird colonies on the Pacific islands emit 13.0 Gg NH_3 $year^{-1}$ from the 29.7 Gg N $year^{-1}$ excreted (P_v = 44 %) (Figure 2).

It is similarly important to note the importance of water availability, both through precipitation and relative humidity is parametrized in the GUANO model. In conditions where NH_3 emission is restricted by low relative humidity e.g. Ascension Island (Riddick et al., 2014), higher precipitation increases the water budget of guano, increasing uric acid hydrolysis rate to form ammonia and ammonium in solution, (Riddick et al., 2017). Hence some water is needed to allow hydrolysis, which in warm locations promotes a high value of P_v. Conversely, in extremely warm dry locations, lack of hydrolysis leads to low P_v values, and an associated build-up of guano. It is therefore no surprise that Pisco on the west coast of Peru, famous for its guano mining industry, is estimated to have a low P_v value (Figure 2) despite high temperatures. In this way, the GUANO model could also be used to simulate the accumulation of guano as a resource and the influence of climate change on this resource.

By contrast, the highest P_v value of any seabird colony in our model was found for on Wake Island in the South Pacific (19.27°N, 166.64°E), where the annual mean temperature is 27ºC, with an annual average precipitation of 906 mm and relative humidity of 95%. At this a site, the hydrological conditions, modest precipitation and high humidity, means the hydrolysis of the excreted uric acid is maximized, with the high temperatures in turn maximizing the fraction of TAN that volatilizes rather than runs-off into the sea.

<<Insert Figure 2>>

3.3 Simulated effects of climate change on emissions

The application of the GUANO model for 2099 allows the effects of future climate change scenarios to be assessed. A comparison with the 2010 baseline shows that NH_3 emissions could increase substantially through the influence of climate on P_v alone, assuming no change in seabird populations and breeding success (Table 1). Given the associated complexities, however, predicting how seabird populations change in the future with anticipated changes in global climate is beyond the scope of the current study. Using nitrogen excretion rates of 2010, increases in NH_3 emission are estimated here in the region of 22-32 Gg NH_3 $year^{-1}$ for the IPCC Scenarios B1, A1B and A2 (Table 1). This amounts to a

405 climate change driven increase in emissions of around 26 to 39% between 2010
406 and 2099, depending on the scenario used.

407 <<Insert Table 1>>

408 The spatial distribution of increases and decreases to the 2010 estimated values of
409 P_v, based on the worst case (A2) data set is presented in Figure 4. To test the
410 effects of predicted wind speed changes separately from changes to the other
411 variables, the wind speed anomalies were added to the GSOD wind dataset and
412 show that wind speed changes in 2099 have little effect on modelled NH_3
413 emission globally, <5% at colonies with the largest predicted change (Figure 3a).
414 When the A2 anomalies for relative humidity alone are added to the GSOD
415 dataset, the effects on P_v are much larger, ranging from -17% to +22% (Figure
416 3b). The largest estimated increases in P_v associated with future relative humidity
417 are in tropical regions of the world, with P_v increasing by up to 22% on many
418 islands in the Indian and Pacific Oceans (Figure 3b). These are regions where
419 guano mining has been conducted, and even relatively small increases in moisture
420 (relative humidity) to these areas may result in an increase in NH_3 loss at these
421 sites and provide a potential threat to the quality and levels of guano production.

422 <<Insert Figure 3>>

423 Precipitation anomalies can act to either increase or decrease P_v with P_v
424 increasing by up to 130 % at colonies where precipitation decreases, such as
425 Norfolk Island, due to less wash-off (Figure 3c) and decreasing by up to 45 % on
426 Pacific Islands. Increases of P_v between 1 and 10 % are estimated throughout
427 Europe, the Caribbean and the Pacific. P_v decreases (linked to increased
428 precipitation) are estimated for most of the regions with colder climates, including
429 Sub-Antarctic Islands and the Arctic.

430 Increases in P_v are most obvious for the predicted A2 temperature anomalies
431 (Figure 3d). The regions with the largest increases (20 - 29 %) are mainly around
432 the Mediterranean and North East Russia. However, in the coldest regions (Sub-
433 Antarctic and Arctic), there may be little or no increase to P_v

434 When the influence of all A2 climate anomalies together is considered, the largest
435 changes to P_v are predicted for the hottest climates, including the Pacific Islands,
436 Indian Ocean islands, Australia and the Mediterranean (Figure 4). These large
437 increases in P_v are expected by the amplifying effect of temperature and water
438 availability from relative humidity and precipitation. The P_v is not predicted to
439 change substantially in the colder climates of the Sub-Antarctic Islands and
440 around the Antarctic peninsula because of relatively negligible increases in
441 temperature (Supplementary Material Section 6 Figure SM6.1).

442 <<Insert Figure 4>>

443 The effects of climate change on P_v at the largest seabird colonies in the world (by
444 number of seabirds) are shown in Figure 5 and Supplementary Material Section 6
445 Tables SM6.1 and Figure 3 (the location of each of these colonies is presented in
446 Supplementary Material Section 6 Figure SM6.2). Ammonia emissions from the
447 penguin colonies on the Isles Kerguelen and Willis Island are predicted to be
448 largely unaffected by climate change (<5% change), even in the worst-case
449 scenario (A2). This is due to increased precipitation balancing out increased
450 temperatures, as discussed above. At colonies with a large increase in

precipitation (e.g. the colonies on the South Sandwich Islands), NH_3 emissions are predicted to decrease because the increased precipitation is likely to wash excreted nitrogen from the colony before it can be emitted as NH_3. Colonies with predicted temperature increases and precipitation decreases (e.g. the Rockhopper penguin colony on Tristan da Cunha), show the largest predicted increase in NH_3 emissions, due to the coupled effect of a decrease in uric acid wash-off because of decreased precipitation and the increased surface NH_3 concentration. Note that the highest volatilization rate for any major colony shown on Figure 5 is on the Peruvian Island of Lobos de Tierra (6.39 ºS, 80.85 ºW), where 69% of the excreted nitrogen is estimated to be volatilized, increasing in 2099 to 73%. This may be contrasted to guano harvesting areas near Pisco on the west coast of Peru (latitude 14 ºS, Supplementary Material Figure SM6.2) where P_v is estimated to increase from 25% to 56% under between 2010 and 2099, indicating the potential to affect future guano production.

<<Insert Figure 5>>

3.4 Evaluation in comparison with measurements

While the main focus of this paper is on assessing the climate dependence of NH_3 emissions and their potential to change under future climate change scenarios, it is important to reflect on the extent of model validation. While it is not feasible to check the modelled emissions from seabird islands on a global scale, the GUANO model has been subject to verification for a number individual colonies across different climates. This is illustrated in Figure 6, which compares (a) the area-based NH_3 emission value and (b) the P_v value calculated by the GUANO model to matching values derived from measurements. Further details of the site based comparison with measurements and methods used to calculate the uncertainty in emission are provided by Riddick et al. (2014; 2016a; 2017).

In principle, the GUANO model was developed independently of the field measurements, except the habitat correction factors. The GUANO model emission estimates match the measurements more closely than the emission calculated by Riddick et al. (2012) for both area-based emission (R^2 = 0.75, m= 0.80, p-value = 0.057) and P_v (R^2 = 0.91, m= 1.07, p-value = 0.01), as the model accounts for the effect of both thermodynamics and the nitrogen depletion through precipitation events. Where the measured emissions are higher than those calculated by the GUANO model (Ascension Island and the Isle of May), this may reflect that the measurements were taken during the breeding season, which is generally the hottest time of the year and when there is the most available nitrogen, and the GUANO model emissions are the average of a year-round simulation.

Also presented are the area-based NH_3 emission value and the P_v value (Supplementary Material Section 6 Figure SM6.3) calculated by Scenario 1 (bioenergetics model), Scenario 2 (temperature adjusted bioenergetics model) and Scenario 3 (best estimate) of Riddick et al. (2012). Generally, the BE model emission estimates are too high in colder areas (Bird Island and Signy Island) and too low in hotter areas (Michaelmas Cay and Ascension Island) and have poor agreement when compared against area-based emission estimates (R^2 = 0.15, m= -3.94, p-value = 0.52) and P_v (R^2 = 0.45, m= -0.31, p-value = 0.21). This is partially addressed by using the thermodynamic correction of the TABE model,

when compared against area-based emission (R^2 = 0.08, m= -0.51, p-value = 0.64) and P_v (R^2 = 0.92, m= 0.19, p-value = 0.01), however this does not account for the full effects of the meteorology on the biogeochemical processes, i.e. the difference between the P_v for the GUANO and TABE models in Figures SM6.4 and SM5.1 will partly be a result of direct measurement of temperature instead of using an average annual temperature.

<<Insert Figure 6>>

3.5 Uncertainty in input data

The meteorological parameters used as input to the GUANO model are a major source of uncertainty, especially the calculation method for ground temperature. The estimated ground temperature used in the GUANO model is based on average ground temperature variations at the three main field measurement sites of Riddick et al. (2014, 2016a). An uncertainty estimate of ± 2 °C was estimated. This results in an NH_3 emission uncertainty of ± 32 % at best. Additionally, precipitation data may also have some associated uncertainty as the reported precipitation data at many colonies is very low (Supplementary Material Section 5 Figure SM5.3) which may result in either underestimation of NH_3 emission through lack of water to form uric acid or overestimation as not enough run-off is accounted for.

However, another substantial uncertainty in global NH_3 emission is the seabird population estimate (± 36 %) (Riddick et al., 2012). New counting techniques have resulted in increased estimates of seabird populations counted in the most remote regions. For example, remote sensing was used to count Little auks (*Alle alle*) on Northumbria Island, Greenland (Egevang et al., 2003), computer-based analysis was applied to count Macaroni penguins in colour aerial photographs on Bird Island, South Georgia (Trathan, 2007), and super-high resolution satellite imagery was used for a census of threatened albatrosses in remote regions (Fretwell et al., 2017). However, because seabirds are generally difficult to reach and new methods are expensive, a large uncertainty in population estimates remains. Combining the sources of error provides a global best estimate of NH_3 emission from seabird colonies of 82 [37 - 127] Gg NH_3 $year^{-1}$.

3.6 Uncertainties in simulated emissions.

The GUANO model provides a method for calculating NH_3 emission from a range of climates. A major asset of the GUANO model is its relative simplicity. For example, it was easily adapted from a site-based approach (Riddick et al., 2017) to model NH_3 emissions for all colonies globally using hourly time-steps for a two year period. Conversely, the simplicity of the GUANO model does impose some limitations. The model uses basic expressions to calculate vertical dispersion at the colony, while complex local topography will influence wind speeds and local turbulence. To ascertain if complex topography has a large effect on NH_3 emission, the model should be validated with NH_3 emissions from colonies with more complex aerodynamics. While this is likely to affect simulated emissions in cold climates where, as Riddick et al. (2014, 2016a) show, emissions are to some extent wind speed dependent, this is likely to be less important in warm climates which are more strongly affected by variability in temperature and water availability.

Many seabird colonies are low lying (e.g., Michaelmas Cay is only 3.5 m above sea-level) and the potentially volatilizable nitrogen may be washed away by storms washing over the land. Until now, wash-off by storm action (i.e., the combined action of wind and water) has been omitted from the GUANO model, which only includes a simple parametrization as a function of precipitation amount. However, the effect of storms could be modelled with the inclusion of colony height above sea level and a relationship between wind speed and wave height. This would require detailed high-resolution digital elevation data for colonies, as some sites are at risk in their entirety, whereas only the lower parts of steeper sloping sites or cliffs would be at increased risk from storms. The slope of a site would also be a key parameter for calculating wash-off by precipitation during and between breeding seasons. However, the spatial resolution of the global seabird database is currently insufficient for all parts of the globe, with data from some countries not being available at the individual colony level. However, in general, the colonies with the poorest spatial resolution are the smallest colonies with smaller contribution to the total seabird NH_3 emission.

The effects of different forms of precipitation on NH_3 emission are not included in the GUANO model. It could be anticipated that colder forms of precipitation (hail, sleet and snow) could affect the temperature of the system and slow the rate of NH_3 formation. Higher intensity of precipitation events may encourage wash-off, as torrential rain may cause flooding events while a similar volume of drizzle over a longer time period may be absorbed into the surface with less wash-off. Global rate/temperature of precipitation data are not known to exist, but the model could be developed in future iterations to account for cold or intense precipitation events if data were available, or by implementing proxy information such as air temperature.

While it is acknowledged that the GUANO model still has weaknesses in the representation of run-off and wash-off by precipitation and storms, it reproduces measured NH_3 emissions at the study sites well (Figure 6 and Riddick et al., 2017). The further refinements suggested above could help to gain better understanding of NH_3 emissions, particularly in regions with high precipitation and storm frequency, and for exploring the extent to which sea level rise may affect colonies.

In addition to parameterization, there may be further uncertainty the absolute NH_3 emission predicted for 2099 caused by guano build up at the colony that is not accounted for by the GUANO model. For the 2010 scenario at the colonies with guano build up, there is either insufficient water to convert uric acid to TAN or it is not warm enough for the TAN to volatilize. In both cases NH_3 emission does not increase in the 3rd year as the meteorology is repeated, with dry climates remaining dry and cold climates staying cold. For the 2099 scenario the NH_3 emission estimate could be an underestimation at colonies that were dry, but then experience higher precipitation. In these cases, accumulated guano not accounted for by the GUANO model will form "historic" NH_3 from residual guano as well as "present-day" NH_3 from freshly excreted guano. To make a justifiable estimate on the NH_3 emissions from historic guano the model would need to run from at least the present day. The first problem with this is we do not have the processing power to do this as the GUANO model takes 24 hours to run for 1 year. Also, changes in seabird population could lead to incorrect emission estimates as NH_3

emissions from recently abandoned penguin rookeries had similar emissions to that of occupied colonies (Speir and Ross, 1984). In a wet temperate climate, Blackall et al. (2008) found ammonia emissions to return to zero within 1-2 month of birds departing, with no carry-over of guano or emission to the following year. Despite the shortcomings of the 2099 NH_3 emission prediction, the P_v is unaffected by historic guano emissions. The colony specific P_v is presented as a more significant outcome than the absolute emission as the absolute emission will also be affected by our highly uncertain values of seabird population in 2099. Future work could compare simulated surface uric acid or TAN from GUANO with field observations as this could be a useful way to assess how well pre-deposited guano is simulated by the model.

3.7 Implications of the research

3.7.1 Comparison of global emissions with other estimates

It is important to summarize the mains reasons for the differences between the GUANO model estimate of global NH_3 emissions (82 Gg NH_3 $year^{-1}$) and the other published estimates. The present study and its validation by measurements clearly shows that the estimates of Blackall et al. (2007) and Riddick et al. (2012, Scenarios 1 and 3) are too high, which is mainly because volatilization rates in polar regions are limited by cold temperatures with substantial amounts of run-off. In simulating NH_3 emissions from grazing animals, Móring et al. (2016) recently demonstrated a feature that may also be relevant to better understand NH_3 emissions from seabird colonies: lower temperatures lead to smaller instantaneous emissions, but as ammoniacal nitrogen remains at the surface this increases the potential for NH_3 emissions at a later stage, thereby increasing the duration of emissions. In this way, if it were not for other loss pathways and interactions, temperature would not ultimately affect the total amount of NH_3 emitted. It is then the interaction between temperature, emission timescale and other competing processes (such as run-off) that lead, in practice, to temperature dependence of NH_3 emission. In the context of the GUANO model, run-off refers to the leaching of TAN and uric acid into the substrate or lateral transport into the sea and is no longer considered biogeochemically available for NH_3 emission. With cooler conditions, and lower instantaneous NH_3 emissions, this increases the chance that the N_r will be washed off by a precipitation event rather than emitted to the atmosphere.

A major consequence of the lower NH_3 emission calculated in this paper is the change this makes to understanding nitrogen pathways at a colony level. Lindeboom (1984) estimated that the percentage of excreted nitrogen that volatilizes (P_v) could be 80 % at a Macaroni penguin colony on Marion Island (Southern Ocean, 47 °S, 38 °E). By contrast, a value of 1.7 % P_v is estimated for the Macaroni penguin colonies on Bird Island using the GUANO model (54 °S, 38 °W) (Supplementary Material Section 6 Figure SM6.2) which is supported by a measurement-based estimate of 1.8% at the same site. This large difference in P_v cannot be explained by taking into account the 2 °C higher average temperature during the breeding season at Marion Island (NCDC, 2011). In the global GUANO model application we included Marion Island as one of the sites, where the annual P_v value is estimated at 3%, which is consistent with our measurements

and site based simulations at Bird Island. Lindeboom (1984) estimated P_v by comparing nitrogen and phosphorus ratios in fresh excreta to older excreta at the colony, assuming that nitrogen was only lost by volatilization, but did not consider nitrogen loss by run-off, which would explain their over-estimation in P_v for Marion Island.

In contrast to the low P_v for penguin colonies, our measurements found that 67 % of the excreted N_r volatilizes as NH_3 at the seabird colony on Michaelmas Cay (Riddick et al., 2014). This compares with a simulated value using the GUANO model for the measurement period of 82% (Riddick et al., 2014), while our global GUANO model application here for gives an annual average P_v of 69%. Our measurements and modelling thus support the early Lindeboom (1984) estimate, but only in colony situations where volatilization dominates with negligible run-off.

3.7.2 Magnitude and significance of seabird NH_3 emissions

The magnitudes of NH_3 emissions calculated by the GUANO model indicate that seabird colonies represent appreciable local NH_3 sources compared with the better known agricultural sources of NH_3 emissions. For example, a poultry installation of similar NH_3 emission as Michaelmas Cay (8,672 kg NH_3 $year^{-1}$) would house 80,000 birds, with each bird emitting NH_3 at 0.1 kg NH_3 $bird^{-1}$ $year^{-1}$ (Sutton et al., 2011). This is similar to the emission from a cattle feedlot of over 650 animals emitting ~10.4 kg NH_3 $animal^{-1}$ $year^{-1}$ (Sutton et al., 2011). The largest source of NH_3 emission in our global model for 2010 is Baker Island in the South Pacific (0.19°N, 176.48°W), which emits 3.9 Gg yr^{-1} (equivalent to the emissions of 39 million chickens or 375 thousand cattle). For 2099 (Scenario A2), our global model still predicts Baker Island to emit the largest amount of NH_3, but this has increased to 6.7 Gg yr^{-1}.

Wilson et al. (2004) reported that UK seabird colonies in remote regions are significant local sources of NH_3 where other emission sources are scarce. At a global scale, seabird colonies are even more removed from anthropogenic nitrogen sources and in many locations can be considered the only major atmospheric nitrogen deposition source for nearby terrestrial ecosystems. This spatial isolation of seabird NH_3 emissions from anthropogenic sources can be put into context by comparison with the spatial estimates of NH_3 emissions from other sources as included in the EDGAR database (EC-JRC/PBL, 2010). When the 0.1° x 0.1° NH_3 emissions in the EDGAR database are co-located with the seabird NH_3 emissions database at same scale, contributions of NH_3 from seabirds mostly account for more than 99.9 % of NH_3 emissions from all sources within the 0.1° x 0.1° cell where they occur (Supplementary Material Section 7 Figure SM7.1).

3.7.3 Seabirds as a model system to study for global ammonia emissions

Seabirds can be considered as representing a "model system" to study NH_3 emission that can provide insights to understand other sources of NH_3 emission better. Many sources of NH_3, especially in agriculture, are complicated by different management practices, whereas seabird emissions are a natural system, uninfluenced by local differences in management practice. As a result, examination of seabird colonies is especially useful to study the climate dependence of NH_3 emission. In this way, relationships between NH_3 emissions

and meteorology can be identified without complications from several externally varying anthropogenic factors (e.g. ground management, manure management techniques, animal housing practices etc.). The GUANO model application presented here provides a step on the way to developing a comprehensive climate-dependent approach to ammonia emissions modelling (Riedo et al., 2002, Sutton et al., 2013, Riddick et al., 2016b) for which parallel steps are being made in other emission contexts (e.g. Bash et al., 2012, Móring et al., 2016).

The present paper shows that NH_3 emissions from seabird nitrogen are highly dependent on meteorology. While an illustrative range for the most important species is shown in Table SM4.1, the full range between species extends from an average P_v of 0.4 % for Emperor penguins to 68.0 % for the Peruvian tern found in South America (see Table 2). While there are differences in emission processes between seabird excreta and animal manure, the principles of the GUANO model are generic and it could be adapted for different types of excreta, such as poultry litter, animal manure and slurry. These adapted models could be used to investigate the dependence of NH_3 emissions from agricultural sources according to meteorology and in consideration of management differences where such data can be obtained.

<<Insert Table 2>>

3.8 Climate change relationships

The results presented here suggest major spatial changes in the percentage of nitrogen that volatilizes as a result of global climate change. At seabird colonies where the largest temperatures are predicted (e.g., Tristan da Cunha, South Atlantic and Midway Atoll, Pacific Ocean), we estimate that P_v increases (Figure 4). Higher P_v leads to an increase in NH_3 volatilized, and may result in increased plant growth and decreased biodiversity by eliminating nitrogen sensitive plant species (Lindeboom, 1984; Ellis, 2005). However, at seabird colonies where precipitation is also predicted to increase, greater run-off will also offset the increase in temperature. The net result is the expectation of negligible changes to P_v at some locations, e.g. on Willis Island and Isles Kerguelen in the Southern Ocean.

Only a few locations globally are expected to have smaller emissions in 2099 than in 2010 according to Scenario A2. Only 7% of the seabird colonies assessed globally (mainly limited to the Southern Ocean; Figure 4) are predicted to experience a reduction in NH_3 emission. Of this 7%, the largest reduction P_v between 2010 and 2099 (using A2 scenario) was 6.3 % and an average of -1.1%. At these colonies the increase in precipitation was found to more than offset the effect of rising temperatures.

An analysis of average values of the change in simulated P_v from 2010 to 2099 as calculated by the GUANO model shows that average P_v values for seabird species in hot climates are predicted to increase by more than 20 %, such as the Sooty tern and the Common noddy (Table 2). Average P_v values for seabirds in temperate climates, such as the Atlantic puffin, are estimated to increase by nearly 5 %. For seabirds in the cold regions, P_v values are predicted to increase by small amounts or decrease, e.g. a decrease in average P_v of 1.2 % for Macaroni penguins. By contrast, for Macaroni penguins located especially in sub-Antarctic areas where

731 precipitation is expected to increase, a small decrease of 1.2% is predicted (Table
732 2).

733 The GUANO model predictions for 2099 only take climate change into account,
734 while assuming that seabird populations will remain stable at their colonies.
735 However, seabird populations, and hence NH_3 emissions, are also expected to be
736 affected by the changing climate. Predicting future population changes in seabirds
737 in response to anticipated climate change was beyond the scope of the present
738 study, but is also relevant for future scenario development.

739 Some of the global changes expected to affect seabird colonies are sea-level rise
740 (0.23 – 0.51 m for the A2 scenario), an increased frequency of extreme weather
741 events, increased frequency in the El Niño Southern Oscillation and increased sea
742 surface temperatures (IPCC, 2007).

743 Sooty terns nesting on low lying atolls in the Pacific Ocean provide an example of
744 how sea-level rise and an increase in the frequency of extreme weather events
745 may affect breeding grounds of seabirds. Michaelmas Cay is currently 3.5 m
746 above sea-level, but with predicted changes in sea-level and more frequent
747 extreme weather events, this land may not be a viable nesting site in the future.
748 120 days are required between egg-laying and fledging for the species at this site,
749 and changing climate may limit the number of consecutive days the island is
750 above water.

751 An example of the effect of El Niño is the change to the Guanay cormorant
752 populations on the west coast of South America. The El Niño Southern
753 Oscillation occurs when warm water appears off the coast of Peru and results in
754 lower primary production of the oceans (Wyrtki, 1975). Past El Niño events
755 coupled with overfishing have had a large impact on the food chain and resulted in
756 a decrease of the Guanay cormorant population in Peru from 20 million in the
757 1950s (Santander, 1981) to 3 million in 2009 (Birdlife International, 2017).

758 Ongoing changes in populations of penguins may also reflect the impact of
759 changing sea surface temperatures. Higher sea surface temperatures have already
760 reduced sea ice, leading to a reduction in Antarctic krill, a vital food source for
761 penguins in the Antarctic region (Brierly, 2008). Failure in krill recruitment may
762 lead to a decline in penguin populations (Trathan et al., 2007). Adelie penguin
763 populations have decreased over the past 25 years because of a reduction in their
764 food supply (Forcada et al., 2006). However, with the climate becoming milder
765 at these latitudes, the environment is more suited to Gentoo penguins (*Pygoscelis*
766 *papua*), which have increased in numbers (Forcada et al., 2006). These examples
767 illustrate the complexity of forecasting overall changes in NH_3 emissions in future
768 scenarios, if both the direct and indirect effects of climate change on bird
769 populations are taken into account in a model system.

770 It is clear, however, that changes in seabird populations will result in changes to
771 the nitrogen dynamics of the surrounding ecosystems. This especially true for
772 environments where naturally occurring nutrients are scarce, such as in sub-polar
773 or arid tropical climates, where small changes to the amount of seabird-mediated
774 marine nutrients imported to terrestrial ecosystems could result in substantial
775 changes to plant productivity.

776 **4. Conclusions**

This paper has presented the results of simulations using the process based GUANO model to further our understanding of global NH_3 emissions from seabird colonies and how these may alter under climate change. The results present the first global maps of NH_3 emissions from seabird colonies using a dynamic model driven by meteorological conditions. The meteorology driven model of NH_3 emissions allow future scenarios to be predicted of the climate change effect on ammonia emissions from seabirds, expressed both as total NH_3 emission and as a percentage volatilization of the excreted nitrogen (P_v). According to IPCC Scenarios A2, A1B and B2, we estimate annual NH_3 emissions for 2099 of 114, 112 and 104 Gg yr^{-1}, respectively. Although emissions are predicted to decrease at a few locations, where increased precipitation is estimated to outweigh the effect of warmer conditions in increasing emission, overall the global picture is that climate change will tend to increase global ammonia emissions from seabirds by around 20 to 40%, depending on the climate scenario for 2099.

The present study provides a first application of how a process model of ammonia emissions from animals, accounting for diurnal and seasonal dynamics, can be applied at a global scale. In so doing it simultaneously provides a demonstration of how the approach can be used to assess scenarios of future climate change and illustrates the potential of the GUANO model for broader application for other livestock NH_3 emission sources at the global scale.

Acknowledgments

The work described in this paper was supported by grants from the NERC CEH Environmental Change Integrating Fund (ECIF), the NERC thematic programme (GANE) and ongoing NERC National Capability programme. It provides modelling underpinning as a contribution to Activity 1.5 of the International Nitrogen Management System (and the '*Towards INMS*' project), under the overall lead of UN Environment and the International Nitrogen Initiative (INI). Thanks to D. Briggs of British Antarctic Survey (BAS) on Signy for information on meteorology and nesting penguins, and the BAS Bird Island crew for their technical and physical support (BAS CGS grant). Thanks to the CEH coastal seas ecology group and other researchers on the Isle of May, especially to M. A. Newell, M. P. Harris (both CEH), T. Alampo and D. Pickett (both Scottish National Heritage). We are grateful to L. J. Wilson (CEH) for initial work on the seabird database and seabird NH_3 emissions and all contributors that provided data for the seabird database: Birdlife International, E. Woehler (University of Tasmania, Australia), H. Strom (Nordic Seabird Group), Y.Yu (Hong Kong Bird Society), R. Mavor (JNCC, UK), D. Irons (US FWS), Canada's Important Bird Areas, Australian Department for Environment, G. Taylor (Department of Conservation, NZ), P. Yorio (Centro Nacional Patagónico), C. A. Yeap (Malaysian Nature Society), P. Round (Mahidol Unversity), A. Petersen (Icelandic Institute of Natural History), C. Egevang (Greenland Institute of Natural Resources), T. Yamamoto (Japan National Institute of Polar Research), T. Anker-Nilssen (Norwegian Institute for Nature Research), J. Elts (Estonian Ornithological Society), M. Hario (Finnish Game and Fisheries Research), Y. Artukhin (Pacific Institute of Geography), M. Paleczny (UBC), R. Allen (Florida Fish and Wildlife Conservation Commission), C. Kisiel (NJ Fish and Wildlife, USA), M. Gibbons, D. Rosenblatt (both Stony Brook University), S. Cameron

(North Carolina Wildlife Resources Commission), B. Ortego (US FWS Texas), S. Stephensen (US FWS Oregon) and R. Boettcher (VA Game and Inland Fisheries).

References

Anderson, W. B. and Polis, G. A. (1999) Nutrient fluxes from water to land: seabirds affect plant nutrient status on Gulf of California islands. Oecologia, 118, 324-332.

Bash, J. O., Cooter, E. J., Dennis, R. L., Walker, J. T. and Pleim, J. E. (2012) Evaluation of a regional air-quality model with bi-directional NH_3 exchange coupled to an agro-ecosystem model. Biogeosciences 10, 1635–164510.5194/bg-10-1635-2013

Birdlife International (2017) Accessed June 2017. URL was correct at a given date. http://datazone.birdlife.org/home.

Blackall, T. D., Wilson, L. J., Bull, J., Theobald, M. R., Bacon, P. J., Hamer, K. C., Wanless, S. and Sutton, M. A. (2008) Temporal variation in atmospheric ammonia concentrations above seabird colonies. Atmospheric Environment, 42, 6942-6950.

Blackall, T. D., Wilson, L. J., Theobald, M. R., Milford, C., Nemitz, E., Bull, J., Bacon, P. J., Hamer, K. C., Wanless, S. and Sutton, M. A. (2007) Ammonia emissions from seabird colonies. Geophysical Research Letters, 34, 5-17.

Brierley, A. S. (2008) Antarctic Ecosystem: Are deep krill ecologicla outliers or portents of a paradigm shift? Current Biology, 18, 252-254.

Croft, B., Wentworth, G. R., Martin, R. V., Leaitch, W. R., Murphy, J. G., Murphy, B. N., Kodros, J. K., Abbatt, J. P. D., and Pierce, J. R.: Contribution of Arctic seabird-colony ammonia to atmospheric particles and cloud-albedo radiative effect, Nat. Comm., 7, 13444, 2016.

EC-JRC/PBL (2010) Emission Database for Global Atmospheric Research (EDGAR), release version 4.1. Accessed January 2017., European Commission, Joint Research Centre (JRC) / Netherlands Environmental Assessment Agency (PBL). http://edgar.jrc.ec.europa.eu.

Egevang, C., Stenhouse, I. J., Phillips, R. A., Petersen, A., Fox, J. W. and Silk, J. R. D. (2010) Tracking of Arctic terns Sterna paradisaea reveals longest animal migration. Proceedings of the National Academy of Sciences of the United States of America, 107, 2078-2081.

Elliott, H. A. & Collins, N. E. (1982) Factors affecting ammonia release in broiler houses. Transactions of the ASAE, 25, 413.

Ellis, J. C. (2005) Marine birds on land: a review of plant biomass, species richness, and community composition in seabird colonies. Plant Ecology, 181, 227-241.

Forcada, J., Trathan, P. N., Reid, K., Murphy, E. J. and Croxall, J. P. (2006) Contrasting population changes in sympatric penguin species in association with climate warming. Global Change Biology, 12, 411-423.

Fretwell, P. T., Scofield, P. and Phillips, R. A. (2017), Using super-high resolution satellite imagery to census threatened albatrosses. Ibis, 159: 481–490. doi:10.1111/ibi.12482.

Gu, B., Sutton, M. A., Chang, S. X., Ge, Y., and Chang, J.: Agricultural ammonia emissions contribute to China's urban air pollution, Front. Ecol. Environ., 12, 265–266, doi:10.1890/14.WB.007, 2014.

IPCC (2007) Intergovernmental Panel on Climate Change 2007, The Physical Science Basis. Contribution of Working Group I to the Fourth Assessment Report of the IPCC.

IPCC (2013) Climate Change 2013: The Physical Science Basis. In: Stocker, T.F., Qin, D., Plattner, G.-K., Tignor, M., Allen, S.K., Boschung, J., Nauels, A., Xia, Y., Bex, V., Midgley, P.M. (Eds.), Contribution of Working Group I to the Fifth Assessment Report of the Intergovernmental Panel on Climate Change. Cambridge University Press, Cambridge, United Kingdom and New York, NY, USA, p. 1535. http://dx.doi.org/10.1017/CBO9781107415324.

IPCC Data (2017) Intergovernmental Panel on Climate Change - Data Distribution Center. Accessed January 2017 URL was correct at a given date. http://www.ipcc-data.org/.

Lindeboom, H. J. (1984) The nitrogen pathway in a penguin rookery. Ecology, 65, 269-277.

Mann, M. E. and Kump, L. R. (2008) Dire predictions: understanding global warming, DK Publishing.

Móring A., Vieno M., Doherty R.M., Laubach J., Taghizadeh-Toosi A. and Sutton M.A. (2016) A process-based model for ammonia emission from urine patches, GAG (Generation of Ammonia from Grazing): description and sensitivity analysis. Biogeosciences 13, 1837-1861.

NCDC (2011) National Climatic Data Center, Integrated Surface Hourly (ISH) database. https://www.ncdc.noaa.gov/data-access. Accessed January 2017. URL was correct at a given date.

NCEP (2011) National Centres for Environmental Protection / National Center for Atmospheric Research NCEP/NCAR Reanalysis project. Accessed January 2017. URL was correct at a given date. http://www.esrl.noaa.gov/psd/data/reanalysis/reanalysis.shtml.

Nemitz, E., Milford, C. and Sutton, M. A. (2001) A two-layer canopy compensation point model for describing bi-directional biosphere-atmosphere exchange of ammonia. Quarterly Journal of the Royal Meteorological Society, 127, 815-833.

Parton, W. J. and Logan, J. A. (1981) A model for diurnal variation in soil and air temperature. Agricultural and Forest Meteorology, 23, 205-216.

Riddick, S., Dragosits, U., Blackall, T., Daunt, F., Wanless, S., and Sutton, M. A. (2012) Global ammonia emissions from seabird, Atmos. Environ., 55, 312-327.

Riddick S., Dragosits U., Blackall T., Daunt F., Braban, C. F., Tang, Y. S., MacFarlane, W., Taylor, S., Wanless S. and Sutton M.A. (2014) Measurement of

909 ammonia emissions from tropical seabird colonies. Measurement of ammonia
910 emissions from tropical seabird colonies. Atmospheric Environment 89. 35-42.

911 Riddick S., Dragosits U., Blackall T., Daunt F., Newell, M., Braban, C. F., Tang,
912 Y. S., Schmale, J., Hill, P., Wanless, S., Trathan, P. and Sutton M.A. (2016a)
913 Measurement of ammonia emissions from temperate and polar seabird colonies.
914 Atmospheric Environment 134, 40-50.

915 Riddick, S., Hess, P., Mahowald, N. and Ward, D.S. (2016a) The modeled
916 response of terrestrial nitrogen pathways to changes in agricultural nitrogen from
917 1850 to the present using the CESM. Estimate of changes in agricultural terrestrial
918 nitrogen pathways and ammonia emissions from 1850 to present in the
919 Community Earth System Model, Biogeosciences 13, 3397-3426.

920 Riddick, S. N., Blackall, T. D., Dragosits, U., Tang, Y. S., Moring, A., Daunt, F.,
921 Wanless, S., Hamer, K. C., and Sutton, M. A. (2017) High temporal resolution
922 modelling of environmentally-dependent seabird ammonia emissions: Description
923 and testing of the GUANO model, Atmos. Environ., 161, 48-60.

924 Riedo, M., Milford, C., Schmid, M. and Sutton, M.A. (2002) Coupling soil-plant-
925 atmosphere exchange of ammonia with ecosystem functioning in grasslands.
926 Ecological Modelling 158, 83-110.

927 Santander, H. (1981) Patterns of distribution and spawning fluctuations of
928 anchovy and sardines. Boletin del Instituto del Mar de Peru, Vol. extraordinario,
929 180-192.

930 Speir, T. W., and Ross, D. J. (1984) Ornithogenic Soils of the Cape Bird Adelie
931 Penguin Rookeries, Antarctica 2. Ammonia Evolution and Enzyme Activities,
932 Polar Biol., 2, 207-212.

933 Stulen, I., Perez-Soba, M., De Kok, L. J. and Van Der Eerden, L. (1998) Impact of
934 gaseous nitrogen deposition on plant functioning. New Phytologist, 139, 61-70.

935 Sutton, M. A., Erisman J. W., Dentener F. & Möller D. (2008) Ammonia in the
936 environment: From ancient times to the present. Environmental Pollution, 156,
937 583-604.

938 Sutton, M. A., Howard, C. M. and Erisman, J. W. (Eds.) (2011) The European
939 Nitrogen Assessment: Sources, Effects and Policy Perspectives, Cambridge
940 University Press.

941 Sutton M.A., Reis R., Riddick S.N., Dragosits U., Nemitz E., Theobald M.R.,
942 Tang Y.S., Braban C.F., Vieno M., Dore A.J., Mitchell R.F., Wanless S., Daunt
943 F., Fowler D., Blackall T.D., Milford. C., Flechard C.F., Loubet B., Massad R.,
944 Cellier P., Coheur P.F., Clarisse L., van Damme M., Ngadi, Y., Clerbaux C.,
945 Skjøth C.A., Geels C., Hertel O., Wichink Kruit R.J., Pinder, R.W., Bash J.O.,
946 Walker J.D., Simpson D., Horvath, L., Misselbrook, T.H., Bleeker A., Dentener F.
947 &Wim de Vries V. (2013) Toward a climate-dependent paradigm of ammonia
948 emission & deposition. Phil. Trans. Roy. Soc. (Ser. B). 368: 20130166.
949 http://dx.doi.org/10.1098/rstb.2013.0166

950 Trathan, P. N., Forcada, J. and Murphy, E. J. (2007) Environmental forcing and
951 Southern Ocean marine predator populations: effects of climate change and

952 variability. Philosophical Transactions of the Royal Society B-Biological
953 Sciences, 362, 2351-2365.

954 Weber, R. J., McMurry, P. H., Mauldin, L., Tanner, D. J., Eisele, F. L., Brechtel,
955 F. J., Kreidenweis, S. M., Kok, G. L., Schillawski, R. D., and Baumgardner, D.: A
956 study of new particle formation and growth involving biogenic and trace gas
957 species measured during ACE 1, J. Geophys. Res.-Atmos., 103, 16385-16396,
958 1998.

959 Wilson, L. J., Bacon, P. J., Bull, J., Dragosits, U., Blackall, T. D., Dunn, T. E.,
960 Hamer, K. C., Sutton, M. A. and Wanless, S. (2004) Modelling the spatial
961 distribution of ammonia emissions from seabirds in the UK. Environmental
962 Pollution, 131, 173-185.

963 Wyrtki, K. (1975) El-Niño - Dynamic response of equatorial Pacific Ocean to
964 atmospheric forcing. Journal of Physical Oceanography, 5, 572-584.

965 Zhu, R., Sun, J., Liu, Y., Gong, Z. and Sun, L. (2011) Potential ammonia
966 emissions from penguin guano, ornithogenic soils and seal colony soils in coastal
967 Antarctica: effects of freezing-thawing cycles and selected environmental
968 variables. Antarctic Science, 23, 78-92.

969

970 **Table 1 Comparison of global NH_3 emission from seabirds in 2099 to IPCC climate change scenarios**
971 **B1, A1B and A2.**

	2010	B1 2099	A1B 2099	A2 2099
Total NH_3 emission [uncertainty range] ($Gg\ NH_3\ year^{-1}$)	81.8 [37 - 127]	103.7 [48 – 160]	111.6 [51 – 172]	113.8 [52 – 175]
Change from 2010 emission estimate (%)		+26.8	+36.4	+39.1

972

973 **Table 2 Average percentage of nitrogen that volatilizes (P_v) for a range of species. With temperature (T)**
974 **in 2099 (IPCC Scenario A2) and P_v for 2099 (IPCC Scenario A2).**

Species	Average T during breeding 2010 (°C)	Average P_v 2010 (%)	Average T during breeding 2099 (°C)	Average P_v 2099 (%)	Change in average P_v 2010 to 2099 (%)
Emperor Penguin[1,5]	-15.9	0.4	-14.4	0.6	+0.2
Snowy Sheathbill	-2.6	2.2	-1.3	2.1	-0.1
Adelie Penguin	-10.2	2.7	-8.9	3.3	+0.6
Atlantic Puffin	9.1	3.1	11.8	7.7	+4.7
Macaroni Penguin	1.1	4.4	2.5	3.2	-1.2
Brown Noddy	27.1	25.8	32.6	47.4	+21.6
Sooty Tern	27.1	40.7	32.6	60.6	+20.1
Little Black Shag[3]	13.3	10.3	17.5	60.0	+49.7
Peruvian Booby[6]	20.0	65.9	23.6	72.3	6.4
Peruvian Tern[2,4]	21.0	68.0	25.1	62.0	-6.0

975 Notes: [1] Smallest estimated P_v value for a seabird species in 2010. [2] Largest estimated P_v value for
976 a seabird species in 2010. [3] Largest simulated climate change driven increase for a seabird species.
977 [4] Largest simulated climate change driven decrease for a seabird species. [5] Smallest estimated P_v
978 value for a seabird species in 2099. [6] Largest estimated P_v value for a seabird species in 2099.

979

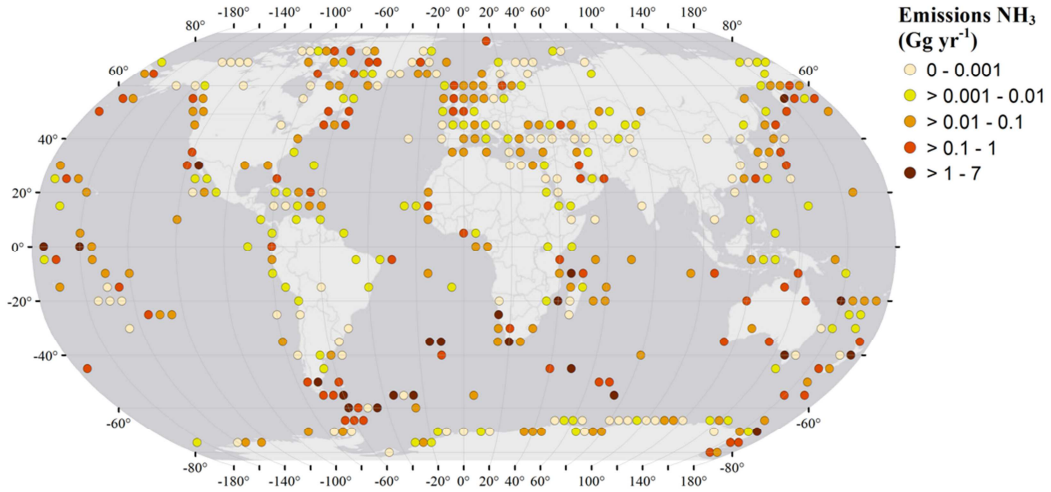

980

981 **Figure 1 Global NH_3 emissions from seabirds aggregated for each 5 degree square, calculated using the**
982 **GUANO model with ground temperature data, for 2010 (baseline).**

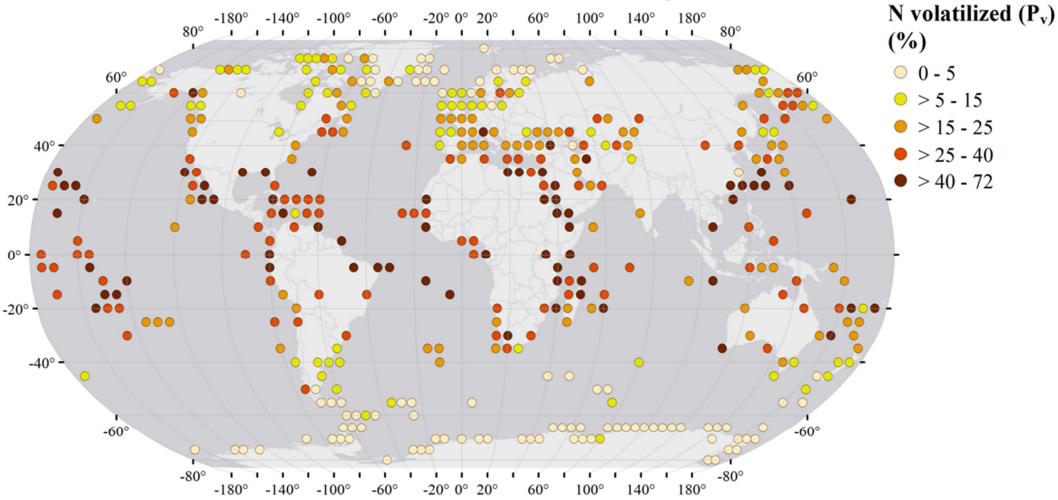

983

984 **Figure 2 Spatial distribution of the percentage of excreted nitrogen that volatilizes (P_v) at seabird**
985 **colonies, calculated using the GUANO model for 2010 (baseline).**

986 a)

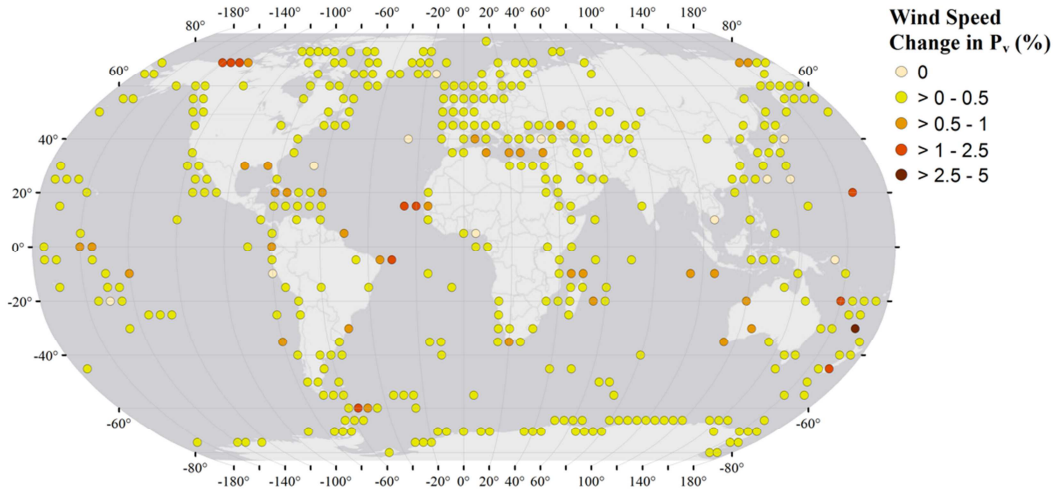

987

988 b)

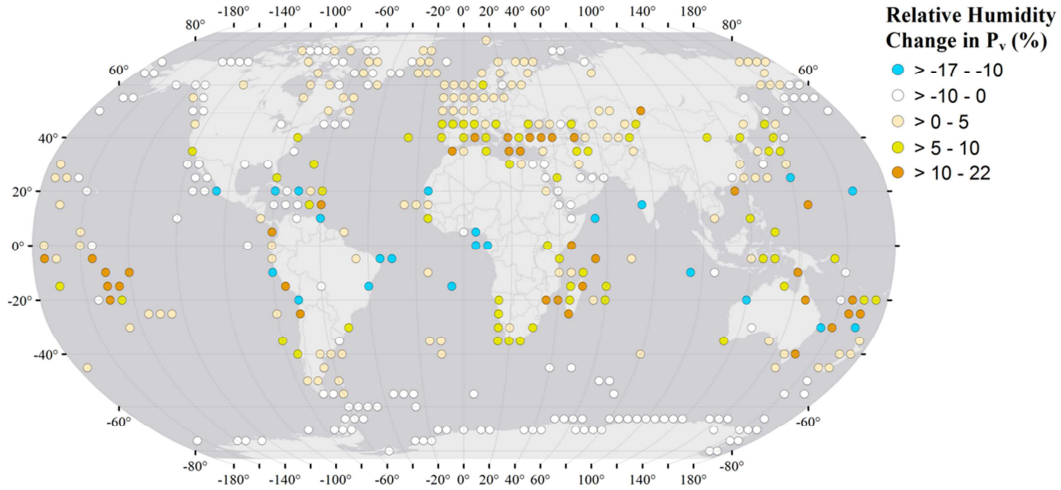

989

990 c)

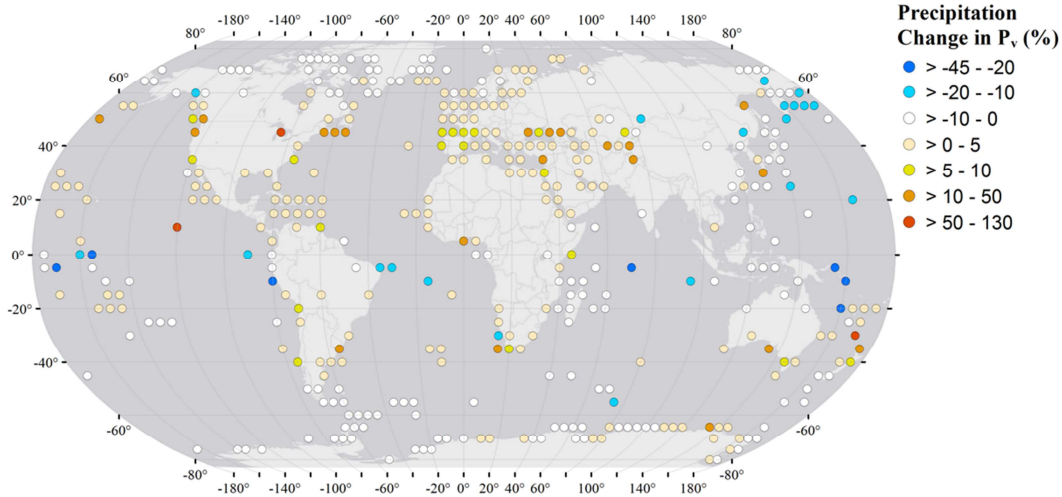

991

992 d)

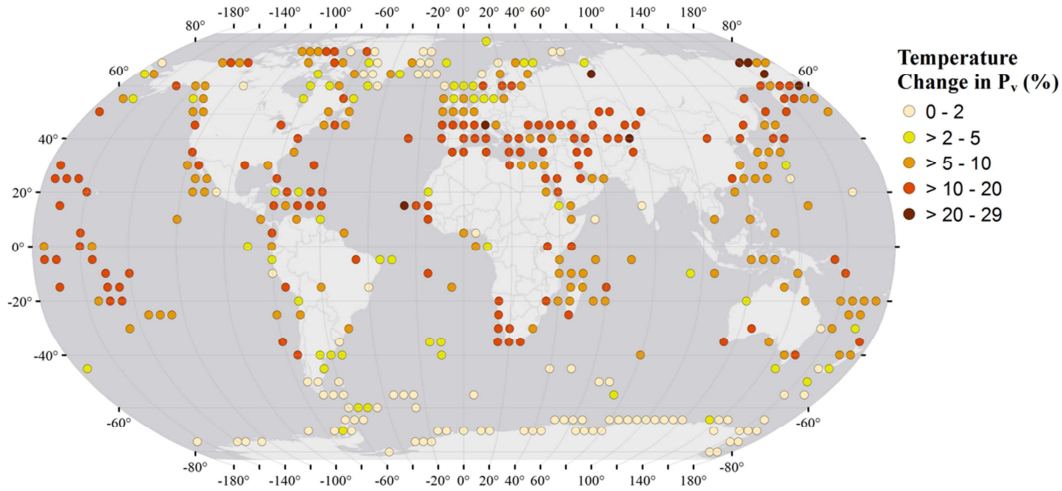

993

994 **Figure 3 Changes to percentage of excreted nitrogen that volatilizes (P_v) estimated between 2010 and**
995 **2099 at seabird colonies when a) wind speed anomalies are considered only, b) relative humidity**

anomalies are considered only, c) precipitation anomalies are considered only and d) temperature anomalies are considered only. Climate anomalies are taken from the IPCC A2 climate change scenario (IPCC DDC, 2011).

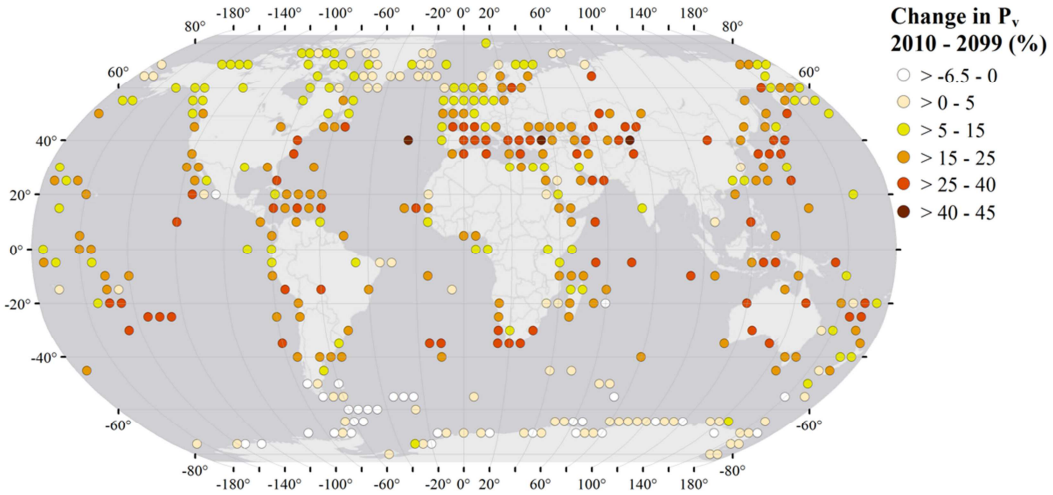

Figure 4 Changes to percentage of excreted nitrogen that volatilizes (P_v) estimated for 2099 at seabird colonies when all climate anomalies are considered, using the IPCC A2 Scenario.

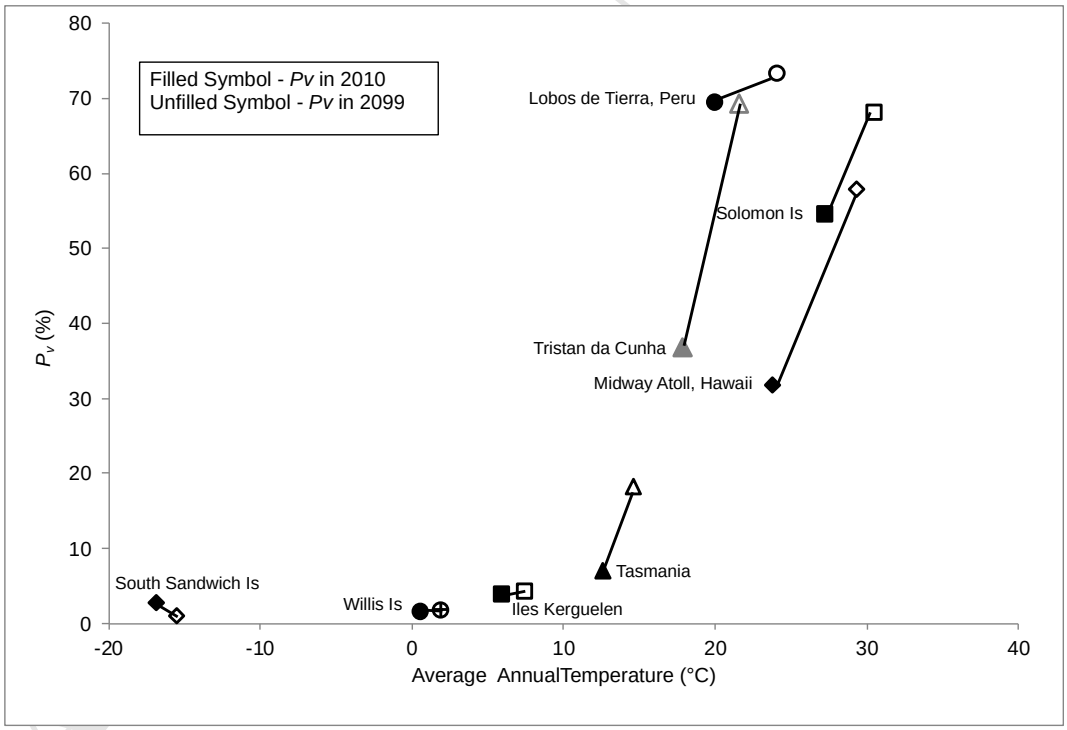

Figure 5 Effects of climate change on *Pv* at the 8 largest seabird colonies, calculated with the GUANO model. Filled symbols indicate NH_3 emissions for 2010 using Global Summary of Day (GSOD); unfilled symbols represent predicted NH_3 emissions by incorporating temperature, wind speed, relative humidity and precipitation anomalies for 2099 (IPCC Scenario A2).

A

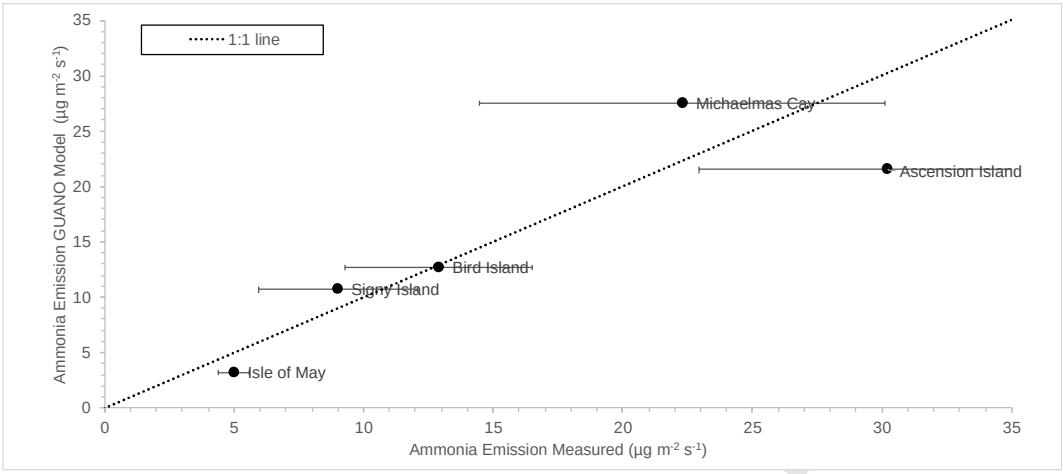

B

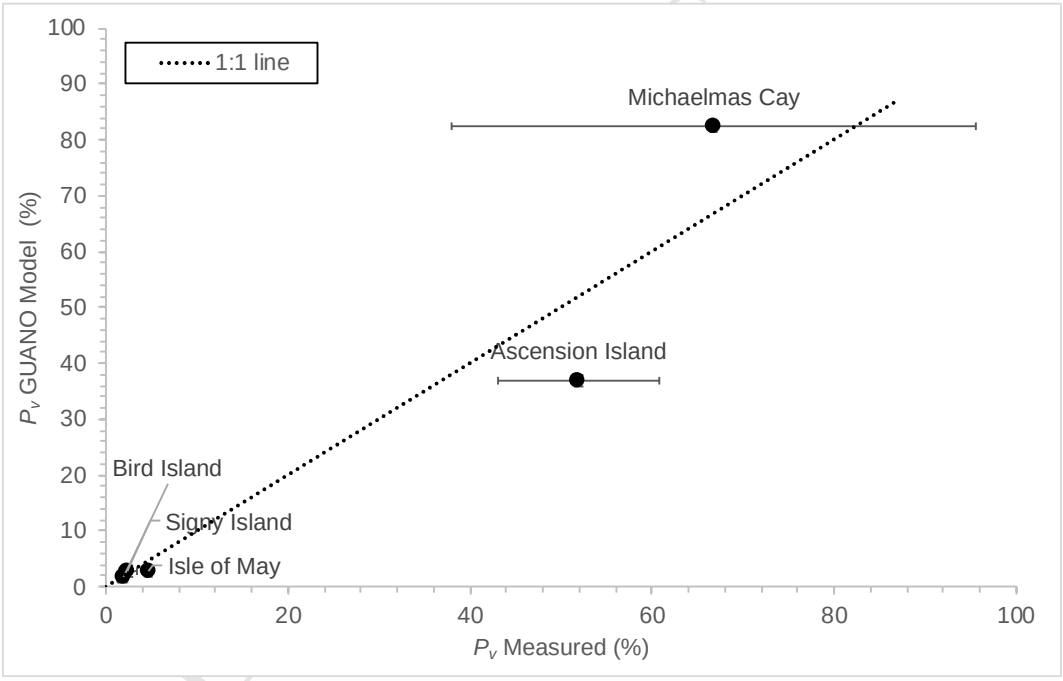

Figure 6 Comparison of (a) the area-based NH_3 emission value and (b) the P_v value calculated by the GUANO model with micrometeorological measured data for site based measurements. Values refer to the periods of the measurements used. For further details see Riddick et al. (2014; 2016a; 2017). Sites: Sooty terns on rocks, Ascension Island (Mid Atlantic); Puffin burrow area with grass, Isle of May (Scotland); Macaroni penguins on rock, Bird Island (South Georgia, South Atlantic); Common noddys on bare ground, Michaelmas Cay (Northern Australia); Chinstrap penguins on bare rock, Signy Island (South Atlantic). Description of the uncertainty analysis used to calculate the error bars presented are found in Riddick et al. (2014; 2016a).

Supplementary Material Section 1: A comparison of the diurnal air temperatures derived from Parton and Logan (1981) with measured values

Figure SM1.1 shows the diurnal variation in air temperature according to the Parton and Logan (1981) model plotted against the measured air temperature data at 2 m above ground level for Ascension Island, the Isle of May and Bird Island. A linear regression shows good agreement between the modelled and measured values for the field sites. The coefficient of determination for each site is shown in Table SM1.1.

Table SM1.1 Comparison between average measured ground temperature and ground temperatures modelled with the Parton and Logan (1982) method, using measured average maximum and minimum air temperature data during the measurement period at each of the field sites.

Field site	Slope	R^2
Isle of May	0.90	0.89
Mars Bay, Ascension	0.88	0.84
Big Mac, Bird Island	0.84	0.79

Although the temperatures calculated by the Parton and Logan (1981) model are serially correlated, the model describes the hourly values of the temperature well in temperate, tropical and polar regions during the seabird breeding season (Figure SM1.1). However, it should be noted that the Parton and Logan (1981) model overestimates temperatures as the temperature increases (dawn) and as it decreases (dusk).

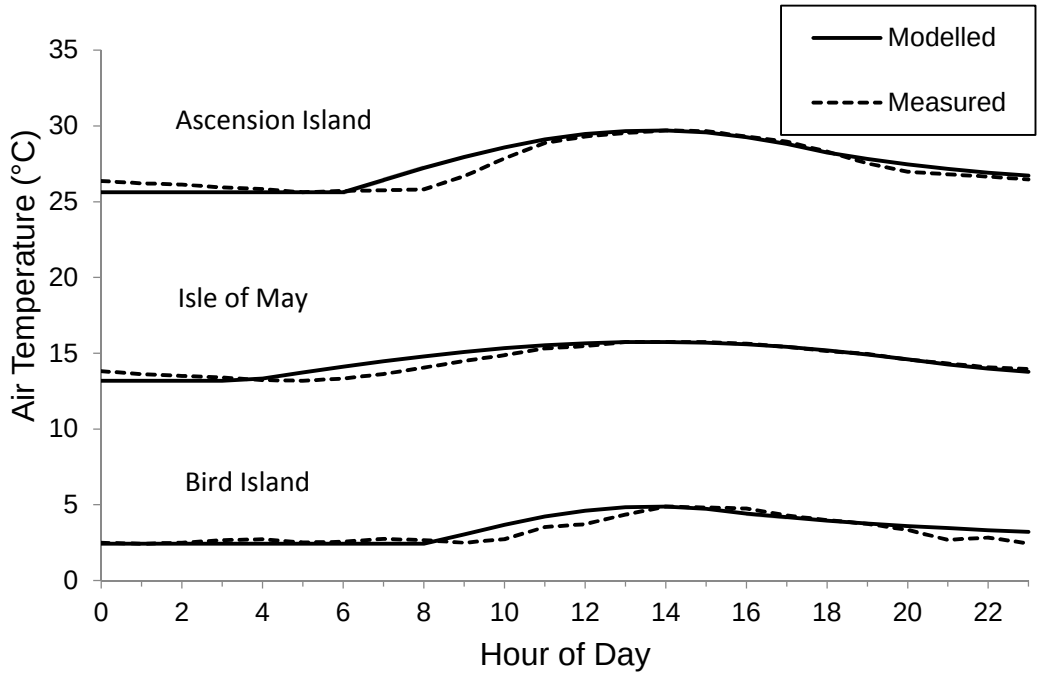

Figure SM1.1 Comparison of the diurnal variation in average measured ground temperature and ground temperatures modelled with the Parton and Logan (1982) method, using measured average maximum and minimum air temperature data during the measurement period at each of the field sites.

Supplementary Material Section 2: Comparison of data from the National Climatic Data Center (NCDC) and Global Surface Summary of the Day (GSOD) data (NCDC, 2011) to the data observed during the measurement campaign of Riddick et al. (2014; 2016a)

To determine the most suitable meteorological dataset for use in the global GUANO model, the detailed meteorological data measured from each field work site were compared with two available global meteorological datasets:

- National Climatic Data Center (NCDC) Global Surface Summary of the Day (GSOD) data (NCDC, 2011) and
- The National Center for Environmental Prediction and the National Center for Atmospheric Research (NCEP/NCAR) reanalysis data set (NCEP, 2011).

The NCDC GSOD data were available as daily data (Integrated Surface Hourly (ISH) dataset), collated by the USAF Climatology Center. The dataset includes observed data from over 9000 meteorological stations globally. A minimum of four observations is used to derive the daily summary data. Due to unit conversions to the metric system, slight rounding errors may occur. Data reports are based on Greenwich Mean Time (GMT). The available data are summarised in Table SM2.1 below:

Table SM2.1 Summary of data available from the National Climatic Data Center (NCDC) Global Surface Summary of the Day (GSOD) (NCDC, 2011)

Variable	Unit	Accuracy
Mean temperature	Fahrenheit	0.1
Mean dew point	Fahrenheit	0.1
Mean visibility	Miles	0.1
Mean Wind Speed	Knots	0.1
Maximum sustained wind speed	Knots	0.1
Maximum wind gust	Knots	0.1
Maximum temperature	Fahrenheit	0.1
Minimum temperature	Fahrenheit	0.1
Precipitation amount	Inches	0.01
Snow depth	Inches	0.1

The NCEP/NCAR data are derived using an analysis/forecast system, which uses weather observations taken by ships, planes, station data and satellite observations. The data are available in 4-times daily (i.e., 6-hourly) format or as daily averages at a 2.5 ° x 2.5 ° grid resolution, and include air temperature at the surface (°C), relative humidity (%), precipitation rate (kg m^{-2} s^{-1}), wind speed (m

s^{-1}), net solar radiation (W m^{-2}) and ground temperature (°C). The largest uncertainty is associated with the air temperature at the surface (or "skin temperature"), which is determined diagnostically as the temperature to balance the fluxes at the surface. The method used to calculate the skin temperature is acknowledged to fail in conditions with low wind speeds and when the thermal exchange coefficient is close to zero (NCEP, 2011). The net solar radiation data are empirically based and take into account cloud cover.

To evaluate the two global datasets for their suitability for estimating global ammonia emissions, meteorological data for the field sites on Ascension, the Isle of May and Bird Island were obtained from both the GSOD and NCEP/NCAR datasets and compared with measured data collected during the field work carried out for this thesis. The NCEP/NCAR data were taken from the grid cell that contained the bird colony, whereas the GSOD data were taken from the meteorological station geographically closest to the bird colony (Table SM2.2).

Table SM2.2 The name and distance of the GSOD meteorological station geographically closest to the bird colony.

Field site	Met station name (NCDC ID #)	Distance between field site and met station (km)
Isle of May	Leuchars Airbase, Fife (31710)	30
Mars Bay, Ascension	Wideawake airhead, Ascension Island (619020)	1
Big Mac, Bird Island	Base Orcadas, Laurie Island, South Orkney Islands (889680)	850

Hourly values of air temperature, relative humidity, wind speed and precipitation were calculated from the GSOD data. Hourly air temperature was calculated using daily maximum and minimum values using the Parton and Logan (1982) method. Hourly values of relative humidity data were taken as the daily average, as were the values for wind speed. The hourly value of precipitation was simply the total daily value divided by 24.

To make a direct comparison between the data sets, hourly values of NCEP/NCAR meteorological data were calculated in the same way as for the GSOD data. The NCEP/NCAR dataset also included ground temperature and net solar radiation data. Hourly ground temperatures were calculated the same way as hourly air temperatures, using the Parton and Logan (1982) model. Net solar radiation during the hours of night was set at zero, where the hours of night were calculated using the method of Parton and Logan (1982). The hourly solar radiation during the day was calculated as the daily average value during the hours of daylight.

To identify which dataset best represents the actual meteorology at the colony, the two sets of hourly data (GSOD and NCEP/NCAR) were compared with the hourly values of meteorological data measured in this study at the three field sites. The quality of fit is determined by calculating the gradient (*m*) and coefficient of

determination (R^2) of the linear regression between measured and GSOD or NCEP/NCAR values, respectively, for each meteorological variable.

GSOD data accord more closely to meteorological data measured at Bird Island, the Isle of May and Ascension Island than NCEP/NCAR data (Tables SM2.3; SM2.4). However, the fit of the GSOD data depends on the proximity of the meteorological station to the seabird colony and also the local conditions (e.g., influence of topography on wind speed/direction). These issues are particularly noticeable by the poor correlation between the GSOD meteorological data measured at Base Orcadas and those measured on Bird Island in the field (R^2 = 0.10 - 0.13), which may be caused by the distance between Base Orcadas and Bird Island (850 km). Despite these differences, the GSOD data are still a better fit to measured data than the NCEP data. The GSOD and NCEP/NCAR precipitation both agree well with measured precipitation data, but the GSOD agrees better with the higher precipitation measured on the Isle of May. The GSOD data for air temperature, relative humidity, wind speed and precipitation are the best available meteorological data, while the NCEP/NCAR provides the best net solar radiation data available. The NCEP/NCAR ground temperature data do not fit well to measured values. The poor fit is due to the large area covered by the 2.5 ° x 2.5 ° grid cells. Each of the three islands occupies only a very small proportion of the respective grid cell, thus the data is more representative of the sea surface temperature rather than the land surface temperature of the grid cell. Therefore, the NCEP/NCAR ground temperature data are not suitable for use in the emission model.

Table SM2.3 Comparison of measured data to Global Summary Of Day (GSOD) data with data measured at the field sites, for the duration of the field work. T_A is air temperature, RH is the relative humidity, WS is wind speed and P is the total precipitation measured during the period of field work. The gradient of the linear regression is denoted as *m* and R^2 is the coefficient of determination between the measurements and the GSOD database.

	Hourly T_A		Hourly RH		Hourly WS		Total P	
	R^2	*m*	R^2	*m*	R^2	*m*	Measured (mm)	GSOD (mm)
Isle of May	0.57	1.3	0.58	0.81	0.40	0.35	110	76
Ascension	0.64	0.80	0.20	0.50	0.10	0.19	6	11
Bird Island	0.10	0.25	0.10	0.22	0.13	0.20	98	76

Table SM2.4 Comparison of measured data for the duration of the field work to National Center for Environmental Prediction and the National Center for Atmospheric Research (NCEP/NCAR) data. T_A is air temperature, T_G is ground temperature, RH is the relative humidity, WS is wind speed, R_n is net radiation and P is precipitation. The gradient of the linear regression is denoted as *m* and R^2 is the coefficient of determination between the measurements and the NCEP/NCAR database.

	Hourly T_A		Hourly T_G		Hourly RH		Hourly WS		Hourly Ir		Total P
	R^2	*m*	R^2	*m*	R^2	*m*	R^2	*m*	R^2	*m*	NCEP/ NCAR (mm)
Isle of May	0.50	0.64	0.01	0.02	0.12	0.47	0.30	0.32	0.45	0.56	62

Ascension	0.06	0.12	0.01	0.01	0.02	0.05	0.02	0.18	0.52	0.60	12
Bird Island	0.03	0.17	0.01	0.02	0.18	0.02	0.03	0.01	0.34	0.40	79

1143

1144

Supplementary Material Section 3: Calculating the temperature offset (T_o) function from air temperature data and surface temperature data from the three field work sites measured during the campaigns of Riddick et al. (2014, 2016a)

Ground temperature is different from air temperature measured at 2 m and has a large influence on NH_3 emission calculations in the GUANO model. Ground temperature is very rarely measured, and as shown above the available NCEP/NCAR dataset had a very poor fit with measured ground temperatures (Table SM2.3). GSOD data provides air temperature in reasonable agreement with measured values (Table SM2.4) and a method for estimating hourly ground temperature values using air temperatures.

Measured ground temperature data for the Isle of May, Ascension Island and Bird Island were used to derive a relationship between ground temperature, air temperature, latitude and time of day. Figure SM3.1 shows the average temperature difference between the air and ground for each hour of the day at the three field sites (Isle of May (56 °N), Ascension (8 °S) and Bird Island (54 °S)) calculated as the mean of each hour during the measurement period.

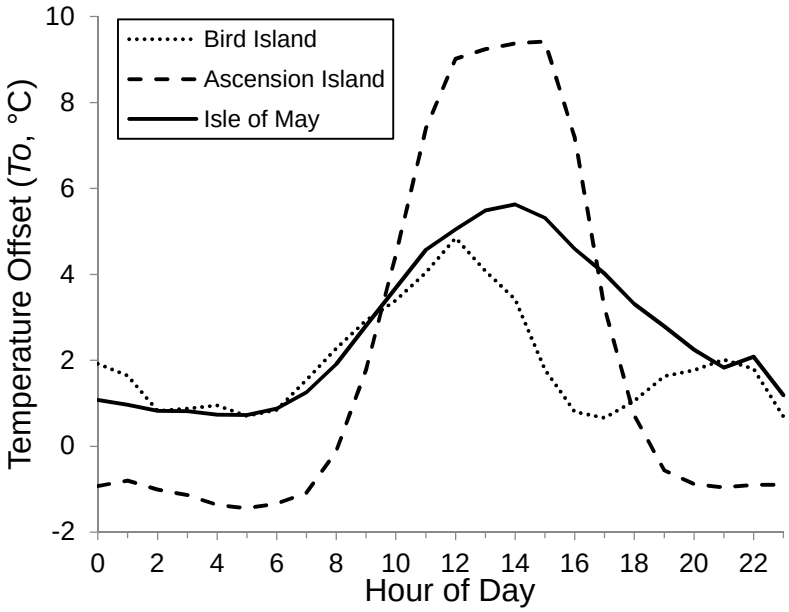

Figure SM3.1 The temperature offset (T_o, °C), difference between average air temperature and ground temperature, for the three field sites during the measurement period (nesting time at each of the colonies): Solid Line: Isle of May (56 °N), Dashed line: Ascension (8 °S) and Dotted Line: Bird Island (54 °S).

Diurnal variation in temperature difference is very similar between the Isle of May and Bird Island, 56 °N and 54 °S, respectively, where the ground is warmer than the air throughout the day and night, with a peak during the middle of the day. The diurnal variation in temperature difference between the air and ground on Ascension is different, with the ground colder than the air during the night and much hotter than the air during the day. Although annual variations occur, the focus here is to provide mean profiles during the bird breeding/nesting seasons.

In the absence of measured global surface temperature data, these were derived from the air temperature for each colony, using measured surface and air temperature data from the three field work sites to parameterize a temperature

offset (T_o) function. T_o was set at the measured values: equator = T_o (Ascension), 55 °N = T_o (Isle of May) and 55 °S = T_o (Bird Island). Using these fixed points, T_o was empirically derived for each hour at any given latitude based on linear interpolation between latitudes for these hourly values, hourly T_0 values calculated using the method presented in Table SM3.1. For sites farther north of the Isle of May and farther south of Bird Island values of these sites were used as limits. Due to the relatively simple derivation method and the limited number of measurement sites, there is substantial uncertainty associated with the estimated surface temperature. Further work to improve estimation of T_0 compared with T_{air} should be considered as part of future work.

Table SM3.1 Empirically derived temperature offset values T_0 for each hour at any given latitude based on linear interpolation of measured data

Hour of Day	Ground Temperature Offset (T_0, °C)
1	$0.0003 \times Latitude^2 - 0.8$
2	$0.0004 \times Latitude^2 - 1.0$
3	$0.0004 \times Latitude^2 - 1.2$
4	$0.0004 \times Latitude^2 - 1.4$
5	$0.0004 \times Latitude^2 - 1.5$
6	$0.0004 \times Latitude^2 - 1.3$
7	$0.0004 \times Latitude^2 - 1.0$
8	$0.0003 \times Latitude^2 - 1.1$
9	$0.0005 \times Latitude^2 + 1.8$
10	$-0.0003 \times Latitude^2 + 4.5$
11	$-0.0007 \times Latitude^2 + 7.5$
12	$-0.0009 \times Latitude^2 + 9.0$
13	$-0.0009 \times Latitude^2 + 9.3$
14	$-0.0009 \times Latitude^2 + 9.5$
15	$-0.0009 \times Latitude^2 + 9.5$
16	$-0.0006 \times Latitude^2 + 7.0$
17	$-0.0001 \times Latitude^2 + 3.0$
18	$0.0002 \times Latitude^2 + 0.7$
19	$0.0003 \times Latitude^2 - 0.5$
20	$0.0003 \times Latitude^2 - 0.8$
21	$0.0003 \times Latitude^2 - 0.9$
22	$0.0003 \times Latitude^2 - 0.9$
23	$0.0003 \times Latitude^2 - 0.9$
24	$0.0004 \times Latitude^2 - 1.0$

Supplementary Material Section 4: A comparison of the NH_3 emission estimates from the GUANO and TABE models

Table SM4.1 Comparison of the NH_3 emission estimates made by the GUANO model (this study) and the TABE model (Riddick et al., 2012 - Scenario 2) and for the ten species with the largest NH_3 emissions, as calculated by the GUANO model.

Species	Model Emission (Gg NH_3 yr^{-1})		Difference in emission
	GUANO model	Scenario 2 TABE model Riddick et al. (2012)	(%)
Macaroni penguin	11.6	17.5	-34
Sooty tern	10.5	4.6	128
Guanay cormorant	8.6	4.9	76
Chinstrap penguin	7.0	4.2	67
Rockhopper penguin	6.7	13.0	-48
Adelie penguin	3.3	1.8	83
King penguin	2.9	10.9	-73
Laysan albatross	2.8	1.2	133
Short-tailed shearwater	2.2	1.2	83
Common guillemot	2.0	1.3	54
Other penguins	1.2	6.7	-82
Other species	11.2	15.8	29
Total	81.8	83.1	
NH_3 emission penguins	42%	65%	

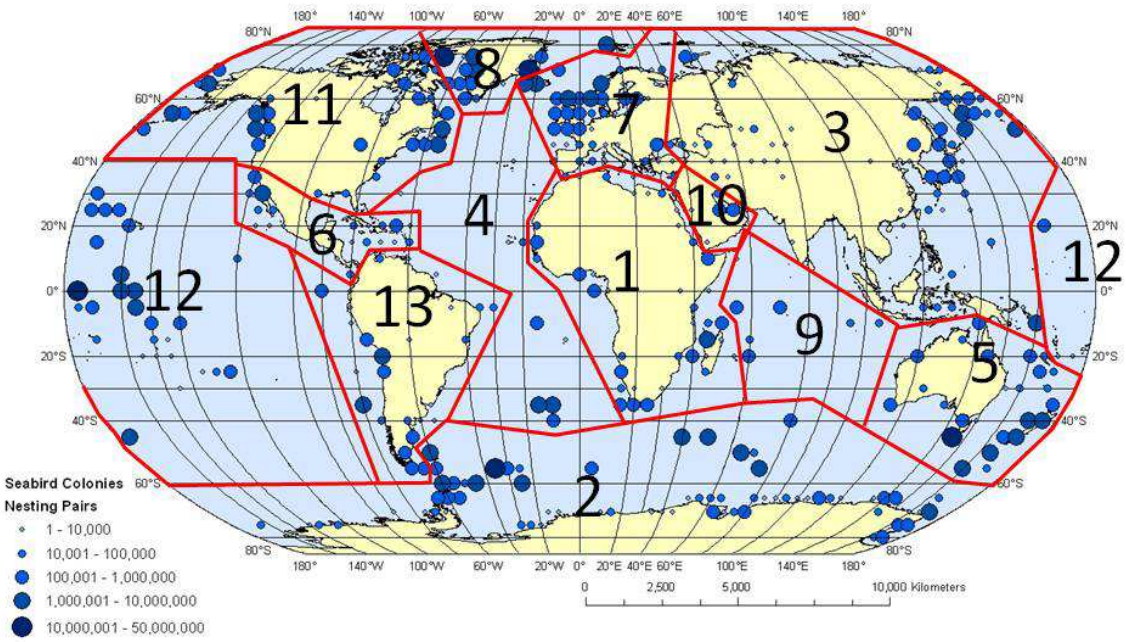

Figure SM4.1 Global distribution of seabird colonies, based on number of breeding pairs. Lines delineate regional boundaries: 1. Africa, 2. Antarctica & Southern Ocean, 3. Asia, 4. Atlantic, 5. Australasia, 6. Caribbean & Central America, 7. Europe, 8. Greenland & Svalbard, 9. Indian Ocean, 10. Middle East, 11. North America, 12. Pacific and 13. South America. To show distribution of the colonies clearly, the number of pairs in each 5° grid square have been summed.

Table SM4.2 Regional NH_3 emission estimates calculated by the GUANO mode1 (using modelled ground temperature) and the Riddick et al. (2012) thermodynamically dependent bioenergetics (TABE) model, Scenario 2.

Region	GUANO Model (Gg NH_3 $Year^{-1}$)	TABE (Scenario 2) (Gg NH_3 $Year^{-1}$)	Differnce in estimated emission (%)
1. Africa	2.59	3.43	-24
2. Antarctica & Southern Ocean	34.2	52.7	-35
3. Asia	6.15	1.06	482
4. Atlantic	0.05	0.02	151
5. Australasia	5.46	3.18	72
6. Caribbean & Central America	1.99	2.40	-17
7. Europe	1.62	2.37	-32
8. Greenland & Svalbard	1.46	2.66	-45
9. Indian Ocean	1.14	0.53	117
10. Middle East	1.19	1.41	-16
11. North America	3.39	1.19	186
12. Pacific	13.0	6.01	117
13. South America	9.55	6.14	55
Total	81.8	83.1	-2

Supplementary Material Section 5: Relationships between GUANO modelled NH_3 emissions and environmental variables

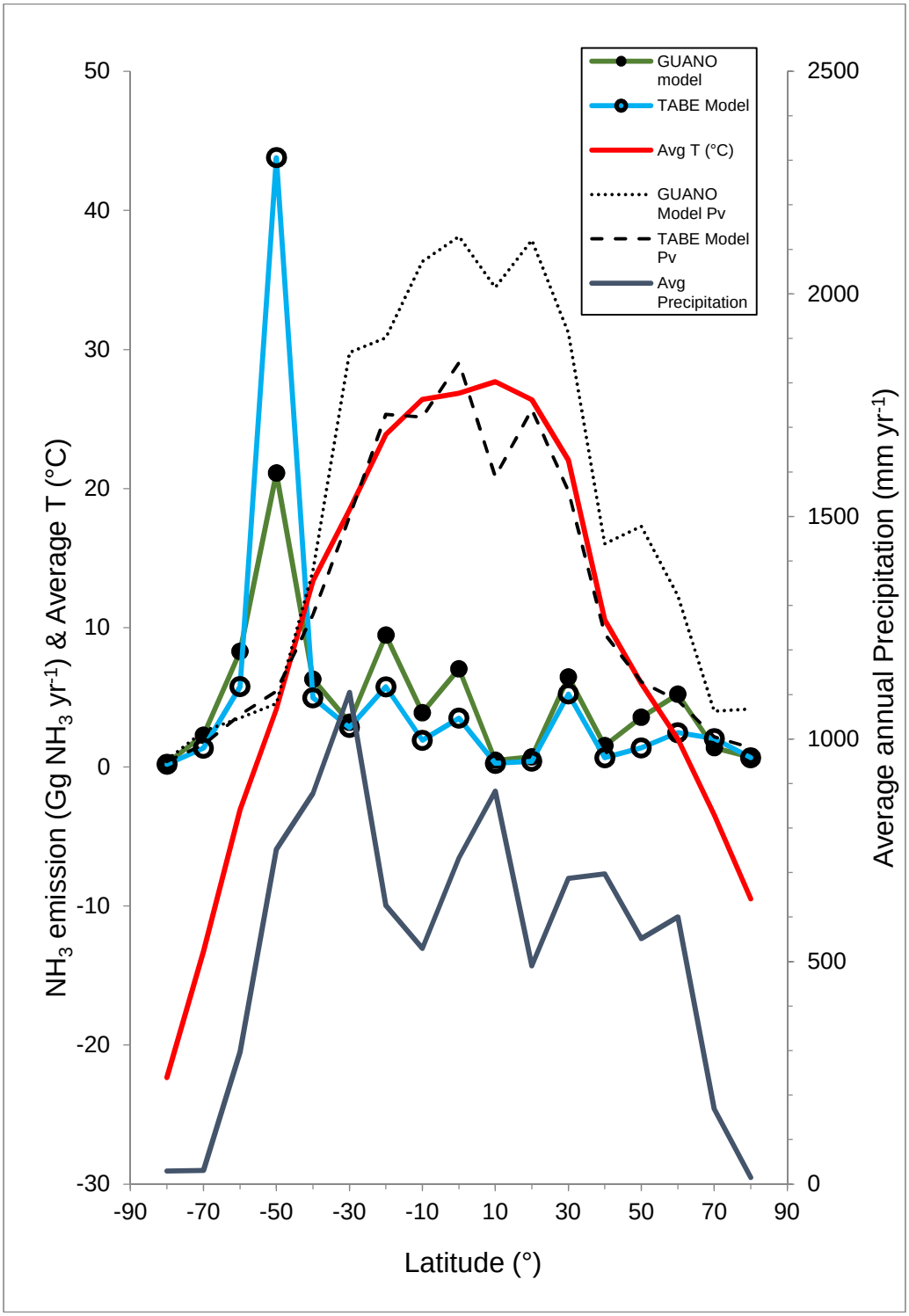

Figure SM5.1 Comparison of the total NH_3 emission estimates made by the Thermodynamically Adjusted BioEnergetics model (TABE, Riddick et al., 2012 - Scenario 2) and the present application of the GUANO model (using modelled values for ground temperature). The average ground temperature and precipitation is also shown and calculated as the average of the hourly values used in the GUANO model at each colony.

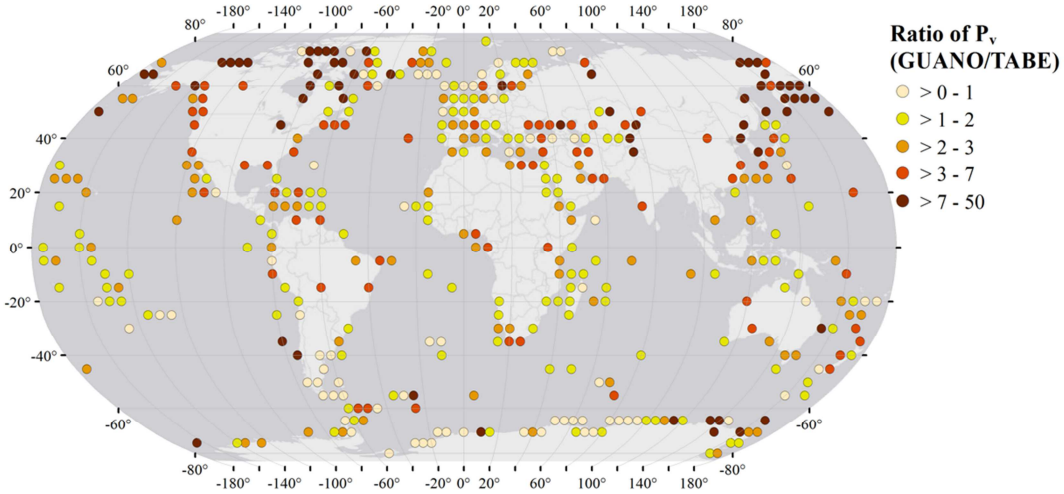

Figure SM5.2 Global map of the ratio: P_v (GUANO)/ P_v (TABE)

Table SM5.1 The product mean correlation coefficient (r) is calculated for each of the variables used in the GUANO model. *RH* denotes average relative humidity during the breeding, *WS* is average wind speed during the breeding season, Total *P* is the annual total precipitation and $T_{breeding}$ is the average temperature during the breeding season.

	RH (%)	*WS* (m s^{-1})	P (mm yr^{-1})
Average $T_{breeding}$	-0.29	-0.08	-0.01
Average *RH*		0.17	-0.10
Average *WS*			-0.02

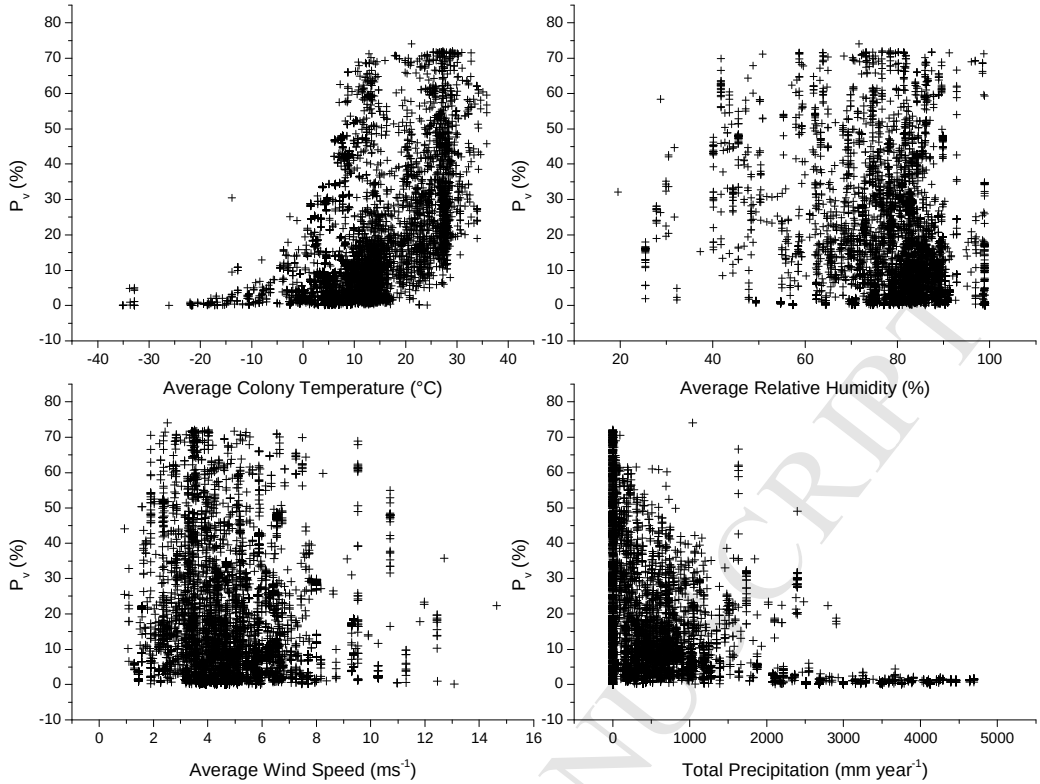

Figure SM5.3 The percentage of nitrogen excreted that volatilizes as NH_3 (*Pv*, %) plotted, for all colonies in the global seabird database, against the total precipitation (mm year^{-1}), the average wind speed during the breeding season (m s^{-1}), the average relative humidity during the breeding season (%) and the average air temperature during the breeding season (°C).

Table SM5.2 Results of a multiple regression analysis of NH_3 emission versus environmental factors in the GUANO model. *RH* denotes relative humidity during the breeding season, *WS* is wind speed during the breeding season, Total *P* is the annual total precipitation and $T_{breeding}$ is the average temperature during the breeding season. The range of the variables denotes the variation globally and ΔPv indicates the difference in *Pv* for one unit change in the variable.

	Average $T_{breeding}$ (°C)	Average *RH* (%)	Average *WS* (m s^{-1})	Total *P* (mm yr^{-1})
Maximum	36	100	11	4700
Minimum	-35	40	1	0
Average	11	89	5	845
ΔP_v per 1 unit of variable (%)	0.97	0.10	0.22	-0.006
p-value	$< 2 \times 10^{-16}$	2.2×10^{-13}	0.003	$< 2 \times 10^{-16}$

Supplementary Material Section 6: Guano modelled NH_3 emission response to a changing climate

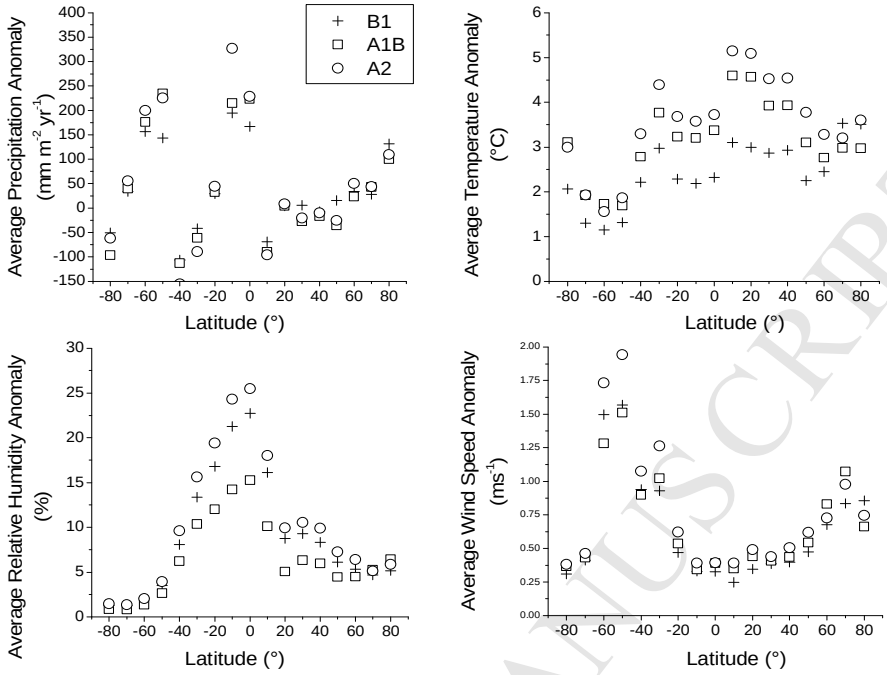

Figure SM6.1 Climate change anomalies for IPCC climate change scenarios B1, A1B and A2 for precipitation, temperature, relative humidity and wind speed.

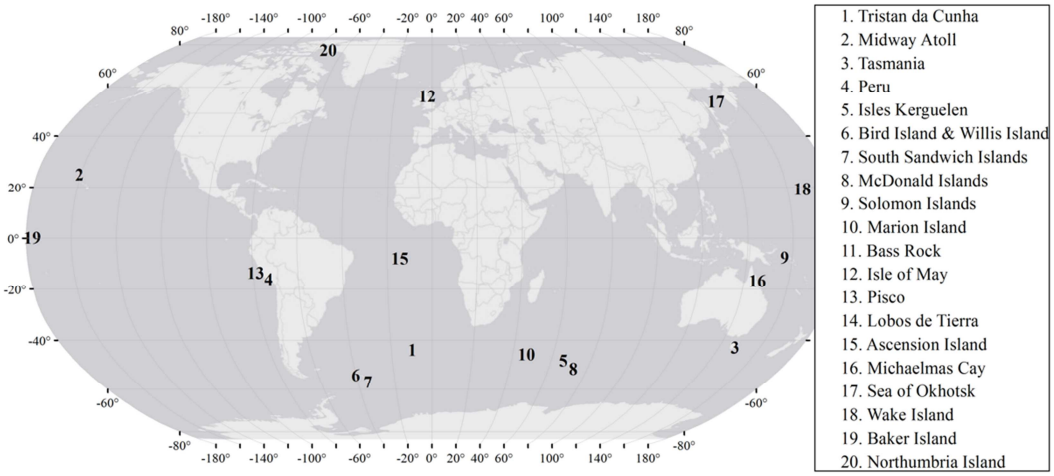

Figure SM6.2 Map of notable seabird colonies discussed in paper

Table SM6.1 Climate change anomalies of IPCC scenario A2 and the predicted change in *Pv* at the largest seabird colonies. Δ*Pv* indicates the change in *Pv* between the 2010 estimates and the predicted values for 2099

Colony	Latitude	A2 Precip Anomaly (mm yr^{-1})	A2 Temp Anomaly (°)	A2 Wind Speed Anomaly (ms^{-1})	A2 Relative Humidity Anomaly (%)	ΔP_v 2010 to 2099 (A2) (%)
Tristan da Cunha	-37	-122.2	3.8	1.9	11.4	32.5
Midway Atoll	28	1.3	5.5	0.4	6.8	26.1

Tasmania	-44	-93.5	2.1	1.5	5.1	11.2
North Coast Peru	-20	-39.8	4.1	0.2	19.7	3.9
Isles Kerguelen	-49	247.4	1.5	2.2	3.0	0.4
Willis Island	-54	278.8	1.4	2.4	2.5	0.2
South Sandwich Is.	-58	258.3	1.4	2.4	2.3	-1.7
McDonald Islands	-53	282.7	1.2	2.8	2.3	-6.5

1253

1254

Table SM6.2 Regional NH_3 emissions (Table A) and P_v (Table B) estimates for GUANO model 2010 and 2099 using all data and individual meteorological anomalies

Part A

EMISSIONS (Gg yr-1)		Future scenarios for 2099				
Region	2010	With 2099 wind anomaly only	With 2099 RH anomaly only	With 2099 PPTN anomaly only	With 2099 Temp anomaly only	2099 with all 4 climate anomalies included.
Africa	2.59	2.61	3.99	2.85	3.62	4.78
Antarctica & Southern Ocean	34.20	35.43	40.32	22.80	42.97	35.08
Asia	6.15	6.19	7.59	4.67	9.26	8.91
Atlantic	0.05	0.05	0.06	0.03	0.06	0.07
Australasia	5.46	5.57	8.25	6.53	7.25	12.52
Caribbean & Central America	1.99	1.99	2.33	1.99	2.70	2.89
Europe	1.62	1.64	2.45	1.68	2.57	3.77
Greenland & Svalbard	1.46	1.47	2.18	1.28	2.50	3.38
Indian Ocean	1.14	1.16	1.78	0.94	1.42	1.94
Middle East	1.19	1.19	1.43	1.23	1.42	1.52
North America	3.39	3.45	4.36	6.06	5.15	6.62
Pacific	13.04	13.11	18.48	9.53	17.38	19.70
South America	9.55	9.57	11.63	10.79	10.77	12.62
Grand Total	81.83	83.43	104.87	70.38	107.07	113.79

1262 Part B.

P_v (%)		Future scenarios for 2099				
Region	2010	With 2099 wind anomaly only	With 2099 RH anomaly only	With 2099 PPTN anomaly only	With 2099 Temp anomaly only	2099 with all 4 climate anomalies included.
Africa	28.1	28.6	40.2	30.1	38.8	47.7
Antarctica & Southern Ocean	4.0	4.1	5.0	3.2	5.2	5.3
Asia	15.8	15.9	21.8	14.2	24.9	28.9
Atlantic	40.4	41.1	57.9	31.6	56.7	68.6
Australasia	23.1	23.6	32.4	28.7	29.2	42.0
Caribbean & Central America	36.9	37.0	47.2	37.5	48.0	56.0
Europe	11.0	11.1	17.5	12.2	17.8	26.9
Greenland & Svalbard	4.1	4.2	5.4	3.4	6.2	7.1
Indian Ocean	29.8	30.2	47.5	24.1	38.4	53.6
Middle East	43.9	44.1	56.0	45.8	56.1	62.9
North America	19.8	19.9	23.6	24.7	27.9	34.1
Pacific	34.6	34.9	48.9	27.2	46.0	53.7
South America	27.2	27.5	30.5	24.0	30.3	33.4
Global Average	6.2	8.6	8.1	6.3	5.3	7.9

1263

A

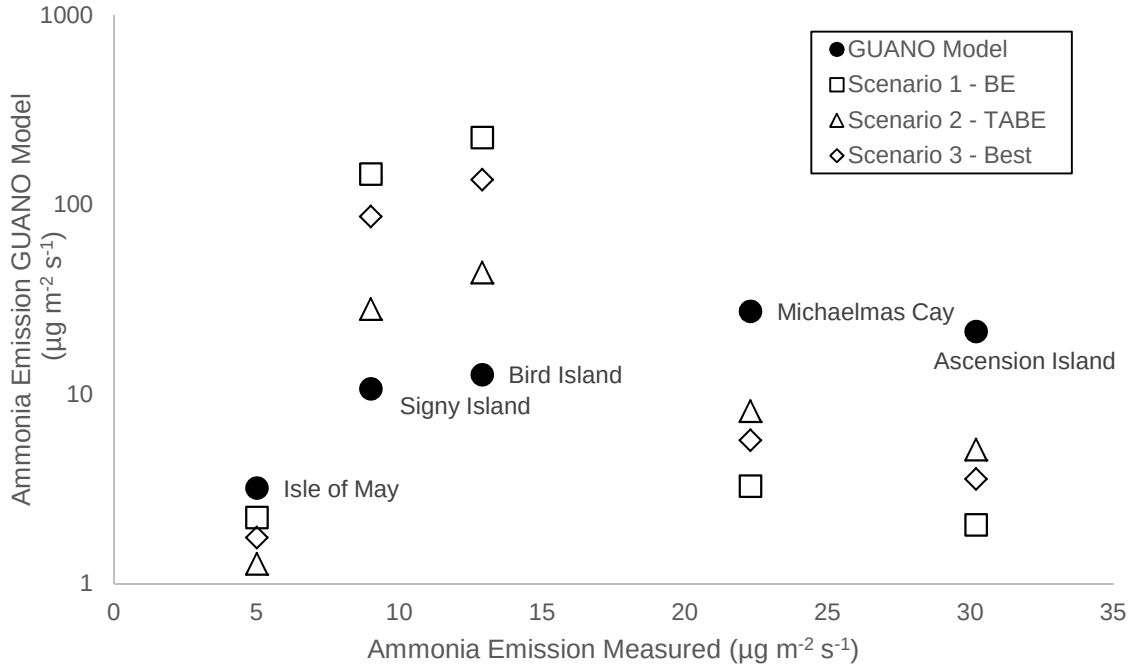

B

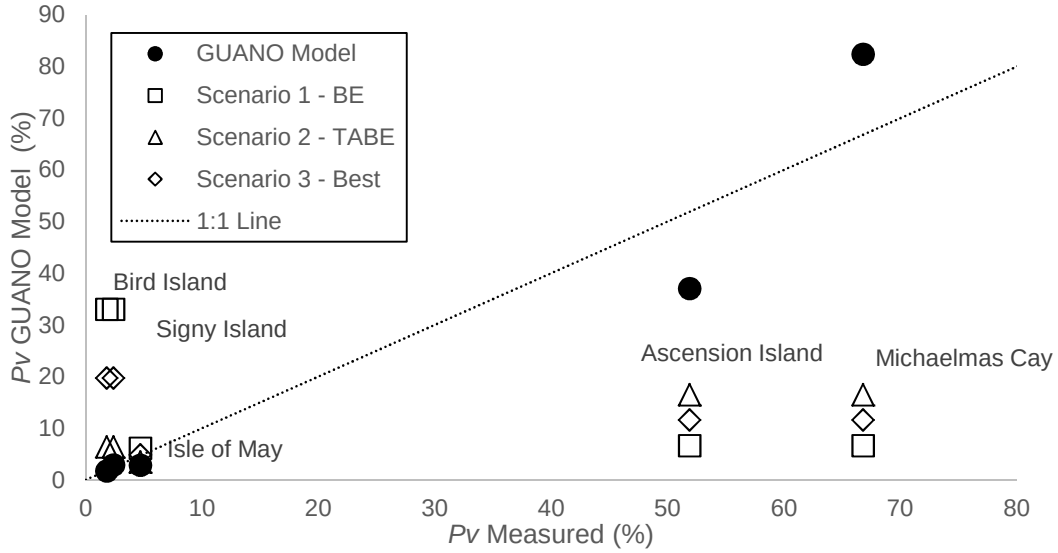

Figure SM6.3. Comparison of (A) the area-based NH_3 emission value and (B) the P_v value calculated by the GUANO model with micrometeorological measured data for site based measurements. Values refer to the periods of the measurements used. For further details see Riddick et al. (2014; 2016a; 2017). Sites: Sooty terns on rocks, Ascension Island (Mid Atlantic); Puffin burrow area with grass, Isle of May (Scotland); Macaroni penguins on rock, Bird Island (South Georgia, South Atlantic); Common noddys on bare ground, Michaelmas Cay (Northern Australia); Chinstrap penguins on bare rock, Signy Island (South Atlantic). Also presented are matching estimates calculated by Riddick et al. (2012): Scenario 1: BE Model, Scenario 2: TABE model and Scenario 3: The best estimate of.

1278 **Supplementary Material Section 7: Contribution of seabird NH_3 emissions as**
1279 **estimated here as a percentage of total NH_3 emissions from seabirds and**
1280 **other sources**

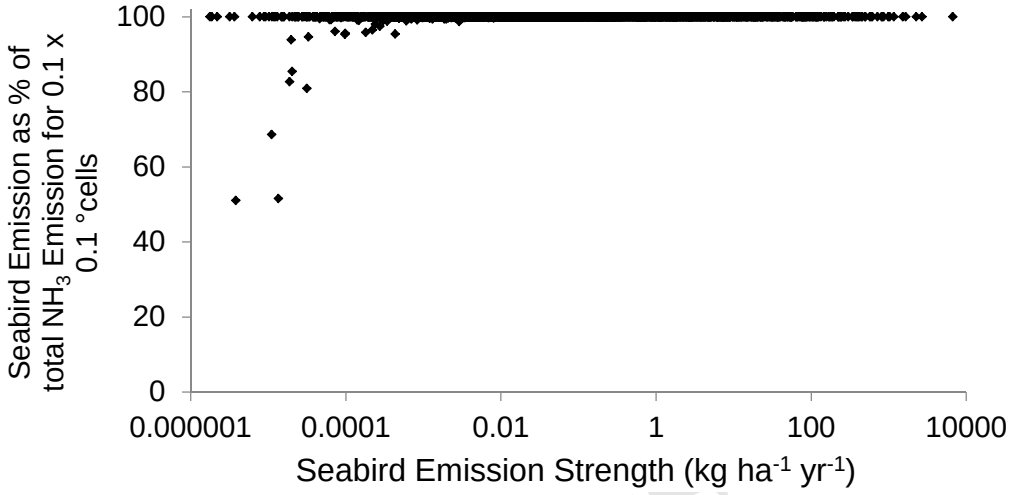

1281

1282 **Figure SM7.1 Contribution of seabird NH_3 emissions as estimated here as a percentage of total NH_3**
1283 **emissions from seabirds and other sources (estimated by the EDGAR database (version 4.1) of EC-**
1284 **JRC, 2010). The figure includes 9,549 dots, where each dot represents a 0.1 by 0.1 degrees square**
1285 **containing at least one modelled seabird colony.**

> Magnitude and distribution of seabird NH_3 emissions globally calculated by a dynamic mass-flow process-based model. > For the year 2010, the total global seabird NH_3 emission is estimated at 82 [37 - 127] Gg $year^{-1}$. > 2010 estimate is less than previously estimated and 82% smaller for the penguin species that breed in high precipitation areas. > The application of IPCC scenarios for 2099 predicted net increase in global seabird NH_3 emissions of 39% (A2 scenario) when compared with the 2010 estimates.

.